Structural Engineering and Mechanics, *Vol. 67, No. 5 (2018) 439-455*
DOI: https://doi.org/10.12989/sem.2018.67.5.439

Probability-based structural response of steel beams and frames with uncertain semi-rigid connections

Dario De Domenico*, Giovanni Falsone[a] and Rossella Laudani[b]

Department of Engineering, University of Messina, Contrada Di Dio, 98166 Sant'Agata, Messina, Italy

(Received March 7, 2018, Revised April 25, 2018, Accepted April 30, 2018)

Abstract. Within a probabilistic framework, this paper addresses the determination of the static structural response of beams and frames with partially restrained (semi-rigid) connections. The flexibility of the nodal connections is incorporated via an idealized linear-elastic behavior of the beam constraints through the use of rotational springs, which are here considered uncertain for taking into account the largely scattered results observed in experimental findings. The analysis is conducted via the Probabilistic Transformation Method, by modelling the spring stiffness terms (or equivalently, the fixity factors of the beam) as uniformly distributed random variables. The limit values of the Eurocode 3 fixity factors for steel semi-rigid connections are assumed. The exact probability density function of a few indicators of the structural response is derived and discussed in order to identify to what extent the uncertainty of the beam constraints affects the resulting beam response. Some design considerations arise which point out the paramount importance of probability-based approaches whenever a comprehensive experimental background regarding the stiffness of the beam connection is lacking, for example in steel frames with semi-rigid connections or in precast reinforced concrete framed structures. Indeed, it is demonstrated that resorting to deterministic approaches may lead to misleading (and in some cases non-conservative) outcomes from a design viewpoint.

Keywords: probability transformation method; probability density function; semi-rigid connections; partially restrained beams; probability-based design

1. Introduction

In conventional analysis and design of framed structures, the behavior of beam-to-column connections is treated as either ideally pinned or perfectly rigid, which circumvents the need of properly accounting for the actual connection stiffness. On the other hand, experimental findings exhibit a broad spectrum of behaviors of the connections in between these two extreme cases, so that *semi-rigid*, or *partially restrained*, connections are more appropriate idealizations (Jones *et al.* 1983, Bjorhovde *et al.* 1990).

Building codes of steel structures such as Eurocode 3 (EC3) (CEN 2005) and the AISC-LRFD Specification (AISC 1994) have long considered semi-rigid connections in addition to rigid and pinned connection. However, the relevance of this topic is not limited to steel framed structures (Chen and Lui 1987, Chiorean 2009, Csébfalvi 2007, Hadianfard and Razani 2003, Sakurai *et al.* 2001, Sekulovic and Salatic 2001, Simões 1996, Thai *et al.* 2016, Zohra and Nacer 2018, Artar and Daloglu 2015, Gorgun and Yilmaz 2012, Esfandyary *et al.* 2015, Hadidi and Rafiee 2014, Katkhuda *et al.* 2010, De Domenico *et al.* 2018) but also apply to other structures, for example precast reinforced concrete structures (Kartal *et al.* 2010, Görgün 1997), steel-braced reinforced concrete frames (Basaga *et al.* 2012), steel-concrete composite frame systems (Nie *et al.* 2011, Faella *et al.* 2008, Amadio *et al.* 2006, Pisano *et al.* 2014, 2015, De Domenico *et al.* 2014), timber-concrete composite beams (Agel and Lokaj 2014), as well as timber structures (Larsen and Jensen 2000). Almost all of the above quoted literature studies were based on the use of *rotational spring stiffness* to characterize the semi-rigid connection, or the *connection percentage*, which is expressed in terms of a so-called "*fixity factor*" (Chiorean 2009, Sekulovic and Salatic 2001, Simões 1996, Thai *et al.* 2016, Kartal *et al.* 2010). The commonly used approach is to incorporate moment-rotation relationships to describe the behavior of the joint, which is generally featured by a *nonlinear* constitutive behavior whose main parameters are calibrated according to experimental data (Jones *et al.* 1983, Chen and Lui 1987, Kishi and Chen 1990).

Experimental testing on the rotational stiffness often leads to a large scatter of measures, even when the same kind of connection is investigated: for instance in (Rauscher and Gerstle 1992) the coefficient of variation of the initial stiffness of double-web angle steel connections was as high as 23%. This indicates that results arising from a deterministic model of the connection may lead to wrong estimates of the actual behavior. Moreover, due to the large scatter of experimental data it is quite difficult for an engineer to decide which value of the rotational stiffness to use, and to assess which consequences such an assumption has in the design process. On the contrary, these questions

*Corresponding author, Ph.D.
E-mail: dario.dedomenico@unime.it
[a]Full Professor
[b]Ph.D. Student

ISSN: 1225-4568 (Print), 1598-6217 (Online)

could be answered by incorporating the randomness of the beam constraints within a *probability-based design approach*. To deal with semi-rigid connections modelled as random variables, various approaches were proposed in the literature: typically, Monte Carlo simulation (MCS) techniques (Thai *et al.* 2016) in conjunction with stochastic finite elements (Hadianfard and Razani 2003, Çavdar *et al.* 2009, Adhikari and Manohar 1999) or the perturbation method (Sakurai *et al.* 2001) were adopted; alternatively, interval analysis is performed in (Tangaramvong *et al.* 2016) to obtain the extreme stochastic response of a semi-rigid frame. However, the accuracy of the approximated results underlying the MCS is strictly related to the number of samples that are generated. Indeed, the probability density function (PDF) of the response is approximated with reasonable accuracy provided that thousands of simulations, not to say millions, are carried out, especially when strongly nonlinear input-output relationships are involved.

Along this research line, in this paper we attempt to characterize, from a probabilistic point of view, the static structural response of an individual beam (which is isolated from a more general framed structure) and of simple frames with partially restrained end nodes. More specifically, we investigate to what extent the uncertainty in the semi-rigid constraints affects the stochastic structural response in terms of a few indicators that are of interest for design purposes, including the element-stiffness-matrix terms, the reactions at the beam ends, the mid-span deflection and the mid-span bending moment. The Probabilistic Transformation Method (PTM), is employed to readily derive the *exact* PDFs of the above response indicators. The PTM, based on a well-known relationship between the PDFs of two vectors of random variables (Papoulis and Pillai 2002), is here resorted to in the peculiar form presented in (Falsone and Settineri 2013a, Falsone and Settineri 2013b). Connection flexibility at the beam ends is incorporated based on a linear approximation, i.e., only the first branch of the actual nonlinear moment-rotation curve is addressed, which is characterized by a constant initial stiffness. The beam fixity factors or connection percentages are treated as uniformly distributed random variables. The analysis of the PDFs of the aforementioned response indicators sheds light on the vital importance of a probability-based approach: indeed, results inferred from deterministic average values, which could be adopted for a preliminary assessment, may lead to misleading estimates of the actual beam response because they are considerably different from the median of the corresponding PDF. More importantly, it is seen that such deterministic average values may in some cases represent non-conservative estimates from a design viewpoint.

Although most of the presented numerical applications refer to steel semi-rigid connections, the present research work is of analytical nature and the discussed approach and analysis method is, in principle, applicable also to other fields, for instance precast reinforced concrete structures, steel-braced reinforced concrete frames, steel-concrete composite frame systems, timber-concrete composite beams, as well as timber structures. Therefore, the aim of the paper is directed towards a general class of engineering problems, not just confined to steel frames.

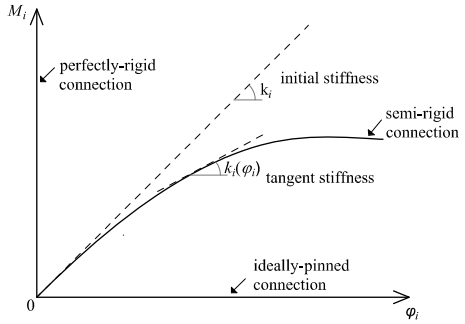

Fig. 1 Typical moment-rotation behavior of rigid and pinned idealizations along with that of semi-rigid beam-to-column connection

2. Deterministic response of beams with semi-rigid nodes

2.1 Beams with semi-rigid end nodes modeled via rotational springs

Typically, framed structures are analyzed and designed considering some idealizations (cf. Fig. 1). For instance, reinforced concrete framed structures are usually treated as frames with perfectly rigid beam-to-column connections, whereas steel framed structures are modelled with ideally pinned connections at the joints. In reality, the moment-rotation relationship of joints is more appropriately and more generally described by semi-rigid (or partially restrained) connections, in that the actual rotational behavior lies in between the two extreme cases of pinned (zero rotational stiffness) and rigid (zero rotation) connection. The partially restrained joints considerably affect the overall moment distributions and displacements of the structure, so that it is of interest to incorporate semi-rigid connections into the model. Accounting for the actual semi-rigid behavior of connections in the design of structures is both realistic and economical, because the redistribution of internal stress leads to more balanced results between the two extreme scenarios of pinned and rigid connections.

An effective and straightforward way to incorporate the characteristics of semi-rigid connections is by means of rotational springs at the beam end nodes. The moment-rotation behavior of the i^{th} joint of a structure is thus modelled either through a constant spring rotational stiffness k_i, thus relying on a linearized model, or via a more complicated nonlinear spring rotational stiffness function $k_i(\varphi_i)$ wherein the *tangent* stiffness depends on the actual value of the rotation experienced by the joint φ_i. In this paper, attention is limited to the former case, in that the partially restraint is featured by a constant spring stiffness k_i. This stiffness represents the so-called *initial* stiffness of the connection that is identified in the first branch of the actual nonlinear moment-rotation curve (i.e., corresponding to reasonably low rotation values, cf. again Fig. 1). These simplifying assumptions restrict the scope of the present

work to structures subjected to static loading. Moreover, due to the linear rotational behavior, the following results and conclusions only apply to serviceability limit states, where the functioning of the structure or structural members under normal use is of interest. Extension to ultimate limit states would be desirable to investigate the probability-based response beyond the elastic limit, for instance in terms of collapse moment or ultimate rotation. This would require extension of the present study by incorporating a nonlinear rotational relation, which is the object of an ongoing research of the authors. With reference to the sketch depicted in Fig. 2, a constant cross-section beam of length L, having moment of inertia *I* and made of a material with Young's modulus *E* is partially restrained at its end nodes 1 and 2 by two rotational springs. The relation between rotations at the beam ends $\varphi_i^{(\mathrm{b})}$ $(i=1,2)$ and rotations of the nodal restraints φ_i $(i=1,2)$ is expressed as

$$\begin{aligned} \varphi_1 - \varphi_1^{(\mathrm{r})} &= \varphi_1^{(\mathrm{b})} = -\left.\frac{dw(x)}{dx}\right|_{x=0}; \\ \varphi_2 - \varphi_2^{(\mathrm{r})} &= \varphi_2^{(\mathrm{b})} = -\left.\frac{dw(x)}{dx}\right|_{x=L} \end{aligned} \tag{1}$$

where $\varphi_i^{(\mathrm{r})}$ $(i=1,2)$ represents the additional, *relative* spring rotation due to the flexibility of the rotational springs and $w(x)$ is the transversal displacement of the beam axis. In the absence of rotational springs, that is in the case of perfectly rigid connections, $\varphi_i^{(\mathrm{r})} \to 0$ and $\varphi_i \equiv \varphi_i^{(\mathrm{b})}$ $(i=1,2)$, and, consequently, the distinction between rotations at the beam ends and rotations at the nodal restraints is meaningless. On the contrary, due to the flexibility of the connection, a relative rotation $\varphi_i^{(\mathrm{r})}$ $(i=1,2)$ is induced by the rotational springs. The bending moment at the beam ends depends on the relative rotations $\varphi_i^{(\mathrm{r})}$ and on the spring rotational stiffness k_i or, equivalently, the spring deformability $\lambda_i=1/k_i$ as follows

$$M_i = -k_i\,\varphi_i^{(\mathrm{r})} = -\frac{\varphi_i^{(\mathrm{r})}}{\lambda_i} \quad (i=1,2) \tag{2}$$

where the minus sign means that the moment reaction at the beam end is opposed to the relative spring rotation. Focusing on the flexural behavior of the beam, we consider the element displacement array $\mathbf{u}^T=[\varphi_1, w_1, \varphi_2, w_2]$. The stiffness matrix of a beam having rotational springs at its ends may easily be constructed by analyzing four loading scenarios in which we impose one displacement at a time equal to one and the remaining three displacements equal to zero. Through the fourth-order beam-bending differential equation, for each loading scenario we compute moment and transversal-force reactions at either nodes, collected in the force array $\mathbf{F}^T=[M_1, V_1, M_2, V_2]$ (cf. again Fig. 2).

The values of the **F** terms form the four columns of the stiffness matrix of the partially restrained beam element $\mathbf{S}(\lambda_1,\lambda_2)$, which depends on the spring deformability λ_i $(i=1,2)$ and can be expressed in the following compact form

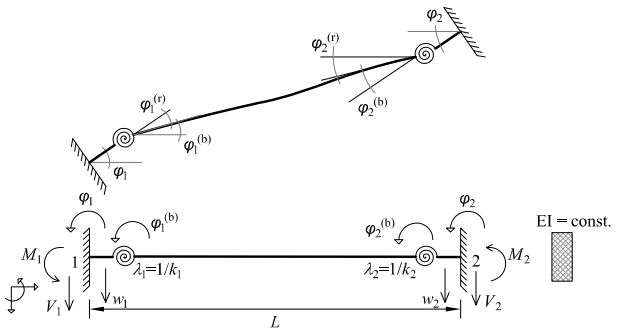

Fig. 2 Sketch and conventions of a beam with partially-restrained (semi-rigid) end nodes

$$\mathbf{S}(\lambda_1,\lambda_2) = \mathbf{S}_r\,\mathbf{S}_c(\lambda_1,\lambda_2) \tag{3}$$

The matrix $\mathbf{S}_r$ entering Eq. (3) is the classical element stiffness matrix of the beam supposed rigid at its end 0, whereas $\mathbf{S}_c(\lambda_1,\lambda_2)$ is a corrective *dimensionless* matrix arising from the flexibility of the connection, which depends on the spring deformability terms λ_1 and λ_2 as follows

$$\mathbf{S}_C(\lambda_1,\lambda_2) = \frac{1}{\Delta(\lambda_1,\lambda_2)}\times \begin{pmatrix} 1+\frac{3EI}{L}\lambda_2 & 1+\frac{2EI}{L}\lambda_2 & 1 & 1+\frac{2EI}{L}\lambda_2 \\ 1+\frac{2EI}{L}\lambda_2 & 1+\frac{EI}{L}(\lambda_1+\lambda_2) & 1+\frac{2EI}{L}\lambda_1 & 1+\frac{EI}{L}(\lambda_1+\lambda_2) \\ 1 & 1+\frac{2EI}{L}\lambda_1 & 1+\frac{3EI}{L}\lambda_1 & 1+\frac{2EI}{L}\lambda_1 \\ 1+\frac{2EI}{L}\lambda_2 & 1+\frac{EI}{L}(\lambda_1+\lambda_2) & 1+\frac{2EI}{L}\lambda_1 & 1+\frac{EI}{L}(\lambda_1+\lambda_2) \end{pmatrix} \tag{4}$$

where the function $\Delta(\lambda_1, \lambda_2)$ is defined as

$$\Delta(\lambda_1,\lambda_2) = 1+\frac{4EI}{L}\left(\lambda_1+\lambda_2\right)+\frac{12(EI)^2}{L^2}\lambda_1\lambda_2 \tag{5}$$

As an example, the first-column terms of the element stiffness matrix $\mathbf{S}(\lambda_1, \lambda_2)$ read

$$\begin{aligned} s_{11} &= \frac{4EI}{L\,\Delta(\lambda_1,\lambda_2)}\left(1+\frac{3EI}{L}\lambda_2\right); \\ s_{12} &= \frac{-6EI}{L^2\Delta(\lambda_1,\lambda_2)}\left(1+\frac{2EI}{L}\lambda_2\right) = -s_{14}; \\ s_{13} &= \frac{2EI}{L\,\Delta(\lambda_1,\lambda_2)} \end{aligned} \tag{6}$$

This format of the stiffness matrix, which is similar to other forms presented in the relevant literature, (e.g., Sekulovic and Salatic 2001, Kartal *et al.* 2010), makes it easy to retrieve the limit cases of a beam with perfectly rigid (clamped) and ideally hinged end nodes by assuming $\lambda_i \to 0$ and $\lambda_i \to \infty$ (i=1,2), respectively. For example, the rotational stiffness at the node 1 is particularized in the following forms

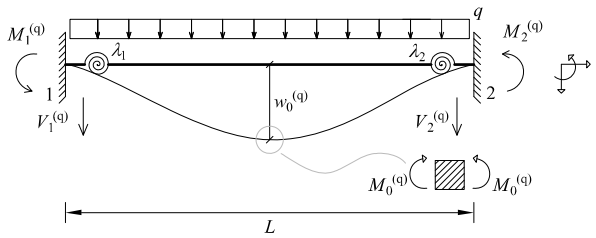

Fig. 3 Beam with partially-restrained (semi-rigid) end nodes subject to a uniformly distributed load

$$\begin{aligned}
&\lim_{\substack{\lambda_1\to 0\\ \lambda_2\to 0}} s_{11} = \frac{4EI}{L} \equiv s_{11\ \text{rigid}};\\
&\lim_{\substack{\lambda_1\to 0\\ \lambda_2\to \infty}} s_{11} = \frac{3EI}{L} \equiv s_{11\ \text{rigid-hinged}};\\
&\lim_{\substack{\lambda_1\to \infty\\ \lambda_2\to \infty}} s_{11} = 0 \equiv s_{11\ \text{hinged}}
\end{aligned} \tag{7}$$

Furthermore, it is of interest to evaluate the nodal actions transmitted to the beam end nodes due to the loads applied along the beam axis, which could be useful for implementation of an automated finite element program. A uniformly distributed transversal load of magnitude q is considered, as sketched in Fig. 3. The fourth-order beam-bending differential equation with the appropriate boundary conditions leads to

$$\begin{aligned}
M_1^{(q)} &= \frac{qL^2}{12}\frac{1}{\Delta(\lambda_1,\lambda_2)}\left(1+\frac{6EI}{L}\lambda_2\right);\\
M_2^{(q)} &= -\frac{qL^2}{12}\frac{1}{\Delta(\lambda_1,\lambda_2)}\left(1+\frac{6EI}{L}\lambda_1\right);\\
V_1^{(q)} &= -\frac{qL}{2}\frac{1}{\Delta(\lambda_1,\lambda_2)}\left(\eta(\lambda_1,\lambda_2)+\frac{2EI}{L}\lambda_2\right);\\
V_2^{(q)} &= -\frac{qL}{2}\frac{1}{\Delta(\lambda_1,\lambda_2)}\left(\eta(\lambda_1,\lambda_2)+\frac{2EI}{L}\lambda_1\right)
\end{aligned} \tag{8}$$

that are the moment reactions and transversal reactions at the end nodes, where the function $\eta(\lambda_1, \lambda_2)$ is defined as

$$\eta(\lambda_1,\lambda_2) = 1+\frac{3EI}{L}(\lambda_1+\lambda_2)+\frac{12(EI)^2}{L^2}\lambda_1\lambda_2 \tag{9}$$

The deterministic limit cases of a rigid, rigid-hinged and hinged beam are retrieved as

$$\begin{aligned}
&\lim_{\substack{\lambda_1\to 0\\ \lambda_2\to 0}} M_1^{(q)} = \frac{qL^2}{12} \equiv M_{1\ \text{rigid}}^{(q)};\\
&\lim_{\substack{\lambda_1\to 0\\ \lambda_2\to \infty}} M_1^{(q)} = \frac{qL^2}{8} \equiv M_{1\ \text{rigid-hinged}}^{(q)};\\
&\lim_{\substack{\lambda_1\to \infty\\ \lambda_2\to \infty}} M_1^{(q)} = 0 \equiv M_{1\ \text{hinged}}^{(q)}
\end{aligned} \tag{10}$$

Finally, we also compute the mid-span moment $M_0^{(q)}$ due to sagging bending

$$\begin{aligned}
M_0^{(q)} &= \frac{qL^2}{24}\times\\
&\frac{1}{\Delta(\lambda_1,\lambda_2)}\left(1+\frac{6EI}{L}(\lambda_1+\lambda_2)+\frac{36(EI)^2}{L^2}\lambda_1\lambda_2\right)
\end{aligned} \tag{11}$$

and the mid-span deflection $w_0^{(q)}$

$$\begin{aligned}
w_0^{(q)} &= \frac{qL^4}{384EI}\times\\
&\frac{1}{\Delta(\lambda_1,\lambda_2)}\left(1+\frac{8EI}{L}(\lambda_1+\lambda_2)+\frac{60(EI)^2}{L^2}\lambda_1\lambda_2\right)
\end{aligned} \tag{12}$$

All these quantities are purposely written as the term related to the fixed beam multiplied by a dimensionless function whose shape is quite similar from variable to variable. Limit cases can easily be retrieved, e.g., concerning Eqs. (11) and (12).

$$\begin{aligned}
&\lim_{\substack{\lambda_1\to 0\\ \lambda_2\to 0}} M_0^{(q)} = \frac{qL^2}{24} \equiv M_{0\ \text{rigid}}^{(q)};\ \lim_{\substack{\lambda_1\to \infty\\ \lambda_2\to \infty}} M_0^{(q)} = \frac{qL^2}{8} \equiv M_{0\ \text{hinged}}^{(q)}\\
&\lim_{\substack{\lambda_1\to 0\\ \lambda_2\to 0}} w_0^{(q)} = \frac{qL^4}{384EI} \equiv w_{0\ \text{rigid}}^{(q)};\ \lim_{\substack{\lambda_1\to \infty\\ \lambda_2\to \infty}} w_0^{(q)} = \frac{5qL^4}{384EI} \equiv w_{0\ \text{hinged}}^{(q)}
\end{aligned} \tag{13}$$

2.2 Frames with semi-rigid end nodes modeled via rotational springs

The analysis is here extended to simple frames with semi-rigid nodes, Fig. 4: two situations are considered, a single-bay frame with semi-rigid beam-to-column connections (frame I) and a single-bay frame with semi-rigid column-to-foundation connections (frame II). Although it could be argued that these frames are too simple, the choice to adopt one-bay and one-floor frames is motivated by convenience reasons: indeed, for these very simple frames, it is easy to derive compact closed-form expressions of the displacements and reactions as explicit functions of the rotational spring deformability terms, which is related to the main focus of the present study. For simplicity, the quantities E, I and L of the beam and of the columns are assumed to be identical. The structural response is easily derived via the displacement method. Neglecting the axial deformations in structural elements, the unknown displacements are collected in the array $\mathbf{u}^T = [\varphi_B, \varphi_C, \delta]$, and the stiffness matrix is expressed as

$$\begin{aligned}
\mathbf{K}^{(\mathrm{I})}(\lambda_1,\lambda_2) &= \begin{pmatrix} s_{11}(\lambda_1,\lambda_2)+\frac{4EI}{L} & s_{31}(\lambda_1,\lambda_2) & \frac{6EI}{L^2}\\ s_{13}(\lambda_1,\lambda_2) & s_{33}(\lambda_1,\lambda_2)+\frac{4EI}{L} & \frac{6EI}{L^2}\\ \frac{6EI}{L^2} & \frac{6EI}{L^2} & \frac{24EI}{L^3}\end{pmatrix}\\
\mathbf{K}^{(\mathrm{II})}(\lambda_1,\lambda_2=0) &= \begin{pmatrix} s_{33}(\lambda_1)+\frac{4EI}{L} & \frac{2EI}{L} & s_{43}(\lambda_1)\\ \frac{2EI}{L} & s_{33}(\lambda_1,\lambda_2)+\frac{4EI}{L} & s_{43}(\lambda_1)\\ s_{34}(\lambda_1) & s_{34}(\lambda_1) & 2s_{44}(\lambda_1)\end{pmatrix}
\end{aligned} \tag{14}$$

wherein S_{ij} is the term of the stiffness matrix $\mathbf{S}(\lambda_1, \lambda_2)$ of the beam element with partially restrained nodes that has been defined in Eqs. (3) and (4). Once the stiffness matrix is constructed, the unknown displacements $\mathbf{u}$ are readily computed via

$$\mathbf{u}^{(i)}(\lambda_1,\lambda_2) = \mathbf{K}^{(i)^{-1}}(\lambda_1,\lambda_2)\mathbf{F}^{(i)}(\lambda_1,\lambda_2) \ \text{ with } \ (i=\mathrm{I},\mathrm{II}). \tag{15}$$

where the force vectors $\mathbf{F}^{(i)}$ for the two frames are given by

$$\mathbf{F}^{(\mathrm{I})}(\lambda_1,\lambda_2)=\begin{bmatrix}0\\0\\P\end{bmatrix}-\begin{bmatrix}M_1^{(\mathrm{q})}(\lambda_1,\lambda_2)\\M_2^{(\mathrm{q})}(\lambda_1,\lambda_2)\\P\end{bmatrix};\quad \mathbf{F}^{(\mathrm{II})}=\begin{bmatrix}0\\0\\P\end{bmatrix}-\begin{bmatrix}qL^2/12\\-qL^2/12\\P\end{bmatrix} \tag{16}$$

For example, the rotation in the node C and the lateral displacement in the frame I are

$$\begin{aligned}&\varphi_C^{(\mathrm{I})}=\varphi_C^{(q,\mathrm{I})}+\varphi_C^{(P,\mathrm{I})}=\frac{1}{\Gamma(\lambda_1,\lambda_2)}\times\\&[\frac{qL^3}{72EI}\left(1+\frac{3EI}{7L}(5\lambda_1-3\lambda_2)\right)+\\&\frac{-PL^2}{28EI}\left(1+\frac{2EI}{3L}(4\lambda_1+7\lambda_2)+\frac{8(EI)^2}{L^2}\lambda_1\lambda_2\right)]\\&\delta^{(\mathrm{I})}=\delta^{(q,\mathrm{I})}+\delta^{(P,\mathrm{I})}=\frac{1}{\Gamma(\lambda_1,\lambda_2)}\times\\&[\frac{qL^3}{84}\left(-\lambda_1+\lambda_2\right)+\\&\frac{5PL^3}{84EI}\left(1+\frac{28EI}{15L}(\lambda_1+\lambda_2)+\frac{48(EI)^2\lambda_1\lambda_2}{15L^2}\right)]\end{aligned} \tag{17}$$

where the superposition principle is resorted to by adding the two separate effects arising from the loads q and P. In (17), the function $\Gamma(\lambda_1,\lambda_2)$ is defined as

$$\Gamma(\lambda_1,\lambda_2)=1+\frac{23EI}{21L}\left(\lambda_1+\lambda_2\right)+\frac{8(EI)^2}{7L^2}\lambda_1\lambda_2 \tag{18}$$

The resulting bending moments at the beam-to-column connection and at the column base are

$$\begin{aligned}&M_B^{(\mathrm{I})}=M_B^{(q,\mathrm{I})}+M_B^{(P,\mathrm{I})}=\\&\frac{1}{\Gamma(\lambda_1,\lambda_2)}\left[\frac{qL^2}{18}\left(1+\frac{6EI}{7L}\lambda_2\right)-\frac{3PL}{14}\left(1+\frac{4EI}{4L}\lambda_2\right)\right]\\&M_D^{(\mathrm{I})}=M_D^{(q,\mathrm{I})}+M_D^{(P,\mathrm{I})}=\frac{1}{\Gamma(\lambda_1,\lambda_2)}\times\\&[\frac{qL^2}{36}\left(1+\frac{3EI}{7L}(-\lambda_1+3\lambda_2)\right)\\&+\frac{2PL}{7}\left(1+\frac{EI}{6L}(10\lambda_1+7\lambda_2)+\frac{2(EI)^2}{L^2}\lambda_1\lambda_2\right)].\end{aligned} \tag{19}$$

In a similar way, the lateral displacement and the bending moments in the frame II are

$$\begin{aligned}&\delta^{(\mathrm{II})}=\delta^{(q,\mathrm{II})}+\delta^{(P,\mathrm{II})}\equiv\delta^{(P,\mathrm{II})}=\\&\frac{1}{\Delta^{(P,\mathrm{II})}(\lambda_1)}\frac{5PL^3}{84EI}\left(1+\frac{18EI}{5L}\lambda_1\right)\\&M_B^{(\mathrm{II})}=M_B^{(q,\mathrm{II})}+M_B^{(P,\mathrm{II})}=\\&\frac{1}{\Delta^{(q,\mathrm{II})}(\lambda_1)}\frac{qL^2}{18}\left(1+\frac{3EI}{L}\lambda_1\right)-\frac{1}{\Delta^{(P,\mathrm{II})}(\lambda_1)}\frac{3PL}{14}\left(1+\frac{2EI}{L}\lambda_1\right)\\&M_D^{(\mathrm{II})}=M_D^{(q,\mathrm{II})}+M_D^{(P,\mathrm{II})}=\\&\frac{1}{\Delta^{(q,\mathrm{II})}(\lambda_1)}\frac{qL^2}{36}\left(1+\frac{3EI}{L}\lambda_1\right)+\frac{1}{\Delta^{(P,\mathrm{II})}(\lambda_1)}\frac{2PL}{7}.\end{aligned} \tag{20}$$

in which the functions $\Delta^{(q,\mathrm{II})}(\lambda_1)$ and $\Delta^{(P,\mathrm{II})}(\lambda_1)$ are given by

$$\Delta^{(q,\mathrm{II})}(\lambda_1)=1+\frac{10EI}{3L}\lambda_1;\ \Delta^{(P,\mathrm{II})}(\lambda_1)=1+\frac{6EI}{7L}\lambda_1 \tag{21}$$

By inspection of Eqs. (17)-(20), it is observed that any variable of the structural response can be expressed as a term related to the perfectly rigid case multiplied by a dimensionless corrective function that depends on the rotational spring deformability of the beams. In the authors' opinion, dealing with more complex, though certainly more realistic, frames with multiple bays and floors, would not add significant insight into the probability-based study here conducted.

The main difference would be related to the slightly more complicated expressions of the displacements and reactions that would arise in this case, which would require finite element discretizations and would make the analysts lose the direct relationship between response and uncertain stiffness factor expressed in a compact manner by the previous equations.

2.3 From the rotational spring deformability to the connection fixity factor

In order to investigate a range of behaviors that are actually representative of semi-rigid connections, attention is now focused on the concept of *fixity factors* (Chiorean 2009, Sekulovic and Salatic 2001, Simões 1996, Thai *et al.* 2016, Kartal *et al.* 2010). It is widely recognized that an estimate of the *initial* stiffness of a joint can be expressed in terms of the element stiffness (related to the Young's modulus E along with the moment of inertia I and the length L of the beam) and a dimensionless fixity factor f as follows

$$k_{\text{joint}}=\frac{4EI}{L}\frac{3f}{4(1-f)} \tag{22}$$

The fixity factor represents the semi-rigid behavior as connection percentage and it varies from 0% for a zero joint stiffness (ideally pinned connection) to 100% when the joint stiffness is infinity (perfectly rigid connection). In the sequel of the paper, attention is focused on steel semi-rigid connections, although the methods presented are not material-specific or element-specific, as already stated in the Introduction. The choice to discuss more in-depth steel semi-rigid connections for the numerical applications is useful to link the present study to a practical problem encountered in the structural analysis of structures with semi-rigid connections. With regard to the steel framed structures, in the Eurocode 3 (CEN 2005) a classification has been established of the fixity factors for pinned, rigid and semi-rigid joints. In particular, the limit values of the fixity factor for pinned and rigid joints are 14% and 89%, respectively (Thai *et al.* 2016). In other words, joints having f<0.14 could be dealt with as pinned, whereas joints with f>0.89 could be approximately described through the perfectly rigid idealization. Some qualitative moment-rotation curves of typical beam-to-column connections in steel structures are shown in Fig. 5(a). Since the present investigation is concerned with semi-rigid connections in general, the analysis discussed below will be extended to the entire interval $f\in[0.14,0.89]$.

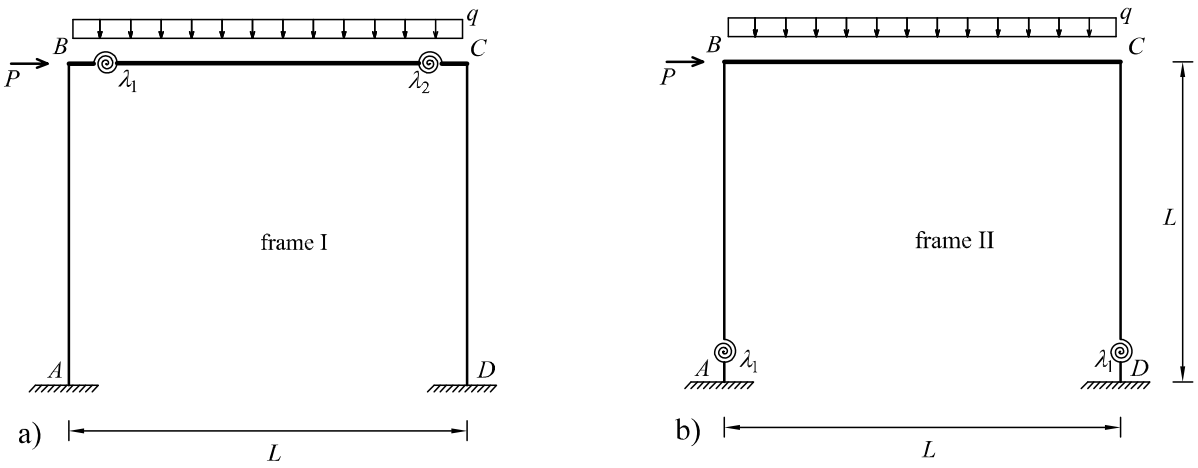

(a) semi-rigid beam-to-column connections (b) semi-rigid beam-to-foundation connections

Fig. 4 Single-bay frame analyzed with different connection types

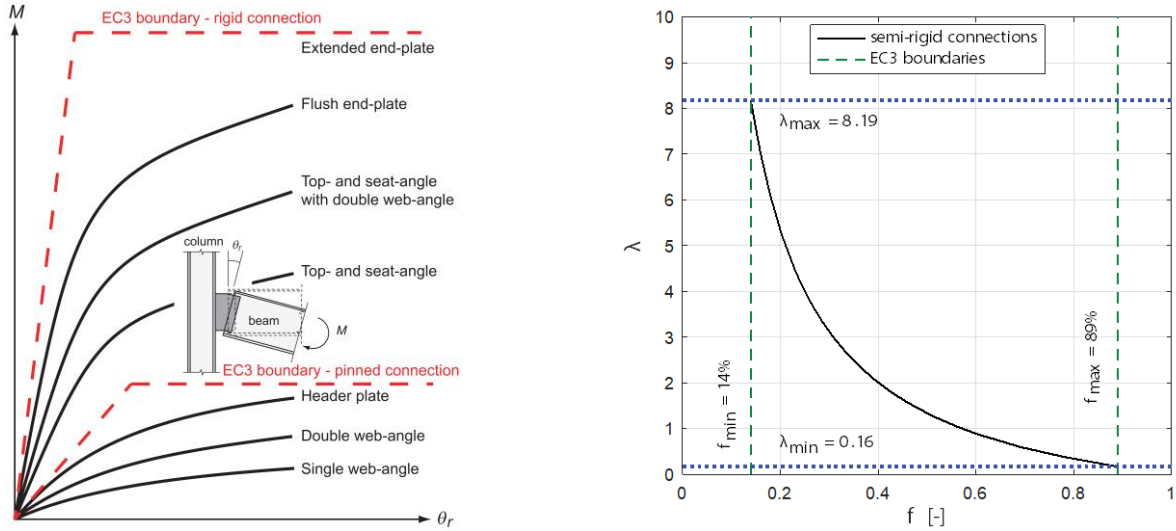

Fig. 5 Moment-rotation curves for various beam-to-column connections along with Eurocode 3 boundaries (adapted from Chen *et al.* (2011) (left) and corresponding rotational spring deformability of the beam (right)

This is reflected by an interval in terms of rotational spring stiffness and, similarly, in terms of rotational spring deformability (normalized with respect to the perfectly rigid case) $\lambda \in [0.16, 8.19]$, the latter depicted in Fig. 5(b). From a probabilistic point of view, if no accurate experimental background is available on the actual beam-to-column connection, the spring deformability of the joint could reasonably be assumed as a uniformly distributed random variable with lower bound and upper bound values equal to 0.16 and 8.19, respectively. This is what is done in the sequel of the paper, although these figures are far from being representative of all the beam-to-column connections.

Obviously, the analyst may decide to deal with a narrower, more realistic interval whenever experimental evidence leads to scattered data whose variability range is reduced as compared to the above one. Indeed, the design scenario is usually determined in terms of a single, or just few connection types involved in a steel frame. In these cases, dealing with a more restricted interval of λ values that is more appropriate for the specific type of connection used (e.g., extended endplate, top-and-seat angle, etc.) is reasonable. Implications of this choice will be briefly outlined in the following sections.

3. The probabilistic transformation method

The probabilistic transformation method (PTM) is based on the probabilistic approach of the space transformation laws of random vectors. In particular, the PTM gives the direct deterministic relationship between the joint PDFs of two random vectors related to each other by the deterministic law corresponding to the assigned space transformation.

Let us consider a n-dimensional random vector $\mathbf{x}$ (input variables), whose joint PDF $p_x(\mathbf{x})$ is known, and let $\mathbf{h}(\cdot)$ be a n-dimensional invertible application with $\mathbf{h}^{-1}(\cdot) = \mathbf{f}(\cdot)$, such that one can write

$$\mathbf{z} = \mathbf{h}(\mathbf{x}); \qquad \mathbf{x} = \mathbf{f}(\mathbf{z}) \tag{23}$$

It is well known that once the direct and inverse relationships in (23) are defined, the joint PDF of the random vector **z** (output variables), that is $p_z(\mathbf{z})$, can easily be obtained through the following expression (Papoulis and Pillai 2002)

$$p_{\mathbf{z}}(\mathbf{z}) = \frac{1}{\left|\det[\mathbf{J}_{\mathbf{h}}(\mathbf{z})]\right|} p_{\mathbf{x}}(\mathbf{f}(\mathbf{z})) \tag{24}$$

where $\mathbf{J}_h(\mathbf{z})$ is the Jacobian matrix associated to the transformation law given in Eq. $(23)_1$

$$\mathbf{J}_{\mathbf{h}}(\mathbf{z}) = (\nabla_{\mathbf{x}}^T \otimes \mathbf{h}(\mathbf{x}))\Big|_{\mathbf{x}=\mathbf{f}(\mathbf{z})} \tag{25}$$

$\nabla_{\mathbf{x}}^T$ being the n^{th} order row-vector operator collecting all the partial derivatives with respect to the components x_i of **x** and the symbol $\otimes$ indicating the Kronecker tensor product (Graham 1981). Expression (24) gives a direct deterministic relationship between the joint PDFs of the random vectors **z** and **x**, which are two scalar functions of multidimensional variables. In other words, the PDF of the output variables $p_z(\mathbf{z})$ can be computed once the PDF of the input variables $p_x(\mathbf{x})$ is known and the transformation law is defined.

A variant of this formulation has been presented in (Falsone and Settineri 2013a). In particular, it is noted that due to Eq. (24) the vectors **x** and **z** should have the same number of components. However, this is not a restriction, as a number of auxiliary variables can be added either to **x** or to **z** in order to balance the vector relationship (Lutes and Sarkani 2004). Another simplification can be introduced when only a marginal PDF of the joint PDF $p_z(\mathbf{z})$ is sought. The traditional way would be performing $n-1$ indefinite integrations of the joint PDF $p_z(\mathbf{z})$ in order to saturate this function with respect to the non-required components, thus isolating the required variable. As a more effective alternative, owing to the properties of the Dirac delta function $\delta(\cdot)$, Eq. (24) is rewritten in the following form

$$p_{\mathbf{z}}(\mathbf{z}) = \int_{-\infty}^{+\infty}\cdots\int_{-\infty}^{+\infty} \frac{1}{\left|\det\left[\mathbf{J}_{\mathbf{h}}(\mathbf{y})\right]\right|} p_{\mathbf{x}}(\mathbf{y})\,\delta(\mathbf{y}-\mathbf{f}(\mathbf{z}))\,\mathrm{d}y_1\cdots\mathrm{d}y_n \tag{26}$$

wherein the multi-dimensional Dirac delta function centered in the point $\mathbf{y}=\mathbf{f}(\mathbf{z})$ is introduced

$$\delta(\mathbf{y}-\mathbf{f}(\mathbf{z})) = \delta(y_1 - f_1(\mathbf{z}))\,\delta(y_2 - f_2(\mathbf{z}))\ldots\ldots\delta(y_n - f_n(\mathbf{z})) \tag{27}$$

The multi-dimensional Dirac Delta introduced above has non-zero value only if $\mathbf{y}=\mathbf{f}(\mathbf{z})$; then, it is equivalent to a multi-dimensional Dirac Delta centered in $\mathbf{z}=\mathbf{f}^{-1}(\mathbf{y})=\mathbf{h}(\mathbf{y})$, provided the determinant of the Jacobian matrix related to the application $\mathbf{h}(\mathbf{y})$ is introduced

$$\delta(\mathbf{y}-\mathbf{f}(\mathbf{z})) = \left|\det\left[\mathbf{J}_{\mathbf{h}}(\mathbf{y})\right]\right|\delta(\mathbf{z}-\mathbf{h}(\mathbf{y})) \tag{28}$$

The determinant of the Jacobian matrix $\mathbf{J_h}$ guarantees that the functions appearing in both sides of Eq. (28) have unitary area. Substituting Eq. (28) into (26) yields

$$p_{\mathbf{z}}(\mathbf{z}) = \int_{-\infty}^{+\infty}\cdots\int_{-\infty}^{+\infty} p_{\mathbf{x}}(\mathbf{y})\,\delta(\mathbf{z}-\mathbf{h}(\mathbf{y}))\,\mathrm{d}y_1\cdots\mathrm{d}y_n \tag{29}$$

We now consider the single component z_j of the output random vector **z** defined by the scalar transformation $z_j = h_j(\mathbf{x})$. The PDF of z_j is readily computed by integrating both sides of Eq. (29) with respect to all the variables z_i, with $i=1,\ldots,n$ and $i \neq j$, thus obtaining

$$p_{z_j}(z_j) = \int_{-\infty}^{+\infty}\ldots\int_{-\infty}^{+\infty} p_{\mathbf{x}}(\mathbf{y})\delta(z_j - h_j(\mathbf{y}))\,\mathrm{d}y_1\cdots\mathrm{d}y_n \tag{30}$$

Eq. (30) is very suitable for defining the single response PDF. In an analogous way, the joint PDF of two components of the output random vector **z** can be obtained as

$$p_{z_j z_k}(z_j, z_k) = \int_{-\infty}^{+\infty}\ldots\int_{-\infty}^{+\infty} p_{\mathbf{x}}(\mathbf{y})\,\delta(z_j - h_j(\mathbf{y}))\,\delta(z_k - h_k(\mathbf{y}))\,\mathrm{d}y_1\cdots\mathrm{d}y_n \tag{31}$$

All the input-output relationships analyzed in this paper involve transformation laws $h_j(\cdot)$ of nonlinear type, because we are dealing with linear structural systems having uncertain parameters (rotational fixity factors). For these cases, the evaluation of the inverse relationship $\mathbf{f}(\cdot)=\mathbf{h}^{-1}(\cdot)$ is not always an easy task, therefore expressions (30) and (31) can be usefully employed in order to compute the PDF of the structural response variables.

4. Probability-based response of beams with semi-rigid nodes

In this Section, we present results concerning the probabilistic structural response, in terms of PDF and cumulative distribution function (CDF), of beams with partially restrained nodes. First, we investigate the uncertainty propagation from the beam end constraints to the elements of the beam stiffness matrix $\mathbf{S}(\lambda_1,\lambda_2)$ reported in (3) and (4). To this aim, based on the probabilistic characterization of the fixity factors as per the EC3 (CEN 2005, Thai *et al.* 2016), discussed above in Section 2.3, we compute the exact PDF of the various terms of the stiffness matrix through the PTM as described in Section 3. The semi-rigid end nodes are modeled via rotational spring deformability that are uniformly distributed random variables within the interval $\lambda \in [0.16, 8.19]$. For the sake of generality, all the variables reported in this study are shown in a dimensionless form by normalizing them with respect to the perfectly rigid case, i.e., the beam with clamped ends (λ=0). As an example, the normalized rotational spring stiffness at the node 1 is expressed as

$$\bar{s}_{11}(\lambda_1,\lambda_2) = \frac{s_{11}(\lambda_1,\lambda_2)}{s_{11\,r}} = \frac{1}{\Delta(\lambda_1,\lambda_2)}\left(1+\frac{3EI}{L}\lambda_2\right) = \frac{\left(1+\frac{3EI}{L}\lambda_2\right)}{1+\frac{4EI}{L}(\lambda_1+\lambda_2)+\frac{12(EI)^2}{L^2}\lambda_1\lambda_2} \tag{32}$$

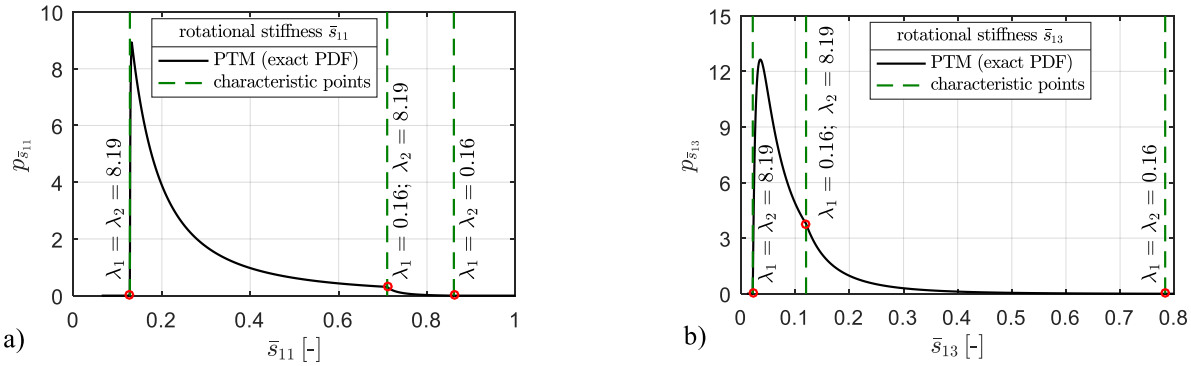

(a) normalized $\bar{s}_{11}$ PDF (b) normalized $\bar{s}_{13}$ PDF

Fig. 6 Qualitative examination of rotational stiffness PDF and characteristic points in partially restrained beams: (a) normalized $\bar{s}_{11}$ PDF; (b) normalized $\bar{s}_{13}$ PDF

where $s_{11}(\lambda_1, \lambda_2)$ is the term reported in $(6)_1$ and $s_{11r} = 4EI / \mathrm{L}$ denotes the rotational stiffness of the corresponding clamped beam. Similar normalizations are employed for all the other terms. Therefore, such dimensionless variables are not affected by the magnitude of the *EI*/*L* ratio and the corresponding PDF and CDF results can be applied to any beam.

In Fig. 6, the PDF of the normalized beam rotational stiffness $\bar{s}_{11}$ and $\bar{s}_{13}$ is depicted. Dealing with semi-rigid connections leads to a narrower interval than [0−1] in the corresponding rotational stiffness: indeed, the extreme value $\bar{s}_{11} \to 1$ (or also $\bar{s}_{13} \to 1$) would be attained for $\lambda_1 = \lambda_2 \to 0$ (beam with perfectly rigid connections), whereas $\bar{s}_{11} \to 0$ (or also $\bar{s}_{13} \to 0$) would be obtained for $\lambda_1 = \lambda_2 \to \infty$ (beam having ideally pinned connections). In particular, it will be seen below that two *characteristic points* are found that represent a lower bound and an upper bound of the two rotational stiffness terms, namely $\bar{s}_{11} \in [0.12772 - 0.86071]$ and $\bar{s}_{13} \in [0.021596 - 0.78327]$. The lower bound is associated with the couple $\lambda_1 = \lambda_2 = 8.19$, while the upper bound is related to couple $\lambda_1 = \lambda_2 = 0.16$. These figures are strictly related to the choice of the interval $\lambda \in [0.16, 8.19]$ made above. It is clearly seen in Fig. 6 that, assuming λ_1 and λ_2 as uniformly distributed random variables, the terms of the beam stiffness matrix are far from being uniformly distributed between their lower bound and upper bound values. This is due to the nonlinear relationship between rotational spring deformability and rotational beam stiffness, cf. Eq. (32). In particular, both the $\bar{s}_{11}$ and $\bar{s}_{13}$ PDF are strongly asymmetrically distributed and are shifted towards the "lower bound case" that resembles an ideally pinned connection $(\lambda_1 = \lambda_2 = 8.19)$. An additional, third characteristic point is identified in the PDF curve as a cusp (red circle in the plot of Fig. 6), which corresponds to the couple λ_1=0.16 and λ_2=8.19. This point may be meant as the semi-rigid counterpart of a clamped-hinged beam idealization. This also explains the reason why such cusp occurs closer to the upper bound case for $\bar{s}_{11}$ (rotational stiffness at the node 1 that is "quasi-rigid") and is located closer to the lower bound case for $\bar{s}_{13}$ (rotational stiffness at the node 2 that is "quasi-hinged").

The implications of such probability-based outcomes in a design process are investigated. To this aim, in Fig. 7 we particularize the qualitative PDF shown in Fig. 6 by computing the median of the distribution. This median may be considered as a reference design value from a probabilistic point of view. Indeed, there is just a probability of 50% that, within the class of semi-rigid connections characterized by the assumed interval $\lambda \in [0.16, 8.19]$, the median is exceeded. It seems reasonable to compare the median with the average value that would be calculated according to a deterministic approach, i.e., the mid-point between the two extreme values (boundaries) corresponding to the two extreme cases of quasi-rigid $(\lambda_1 = \lambda_2 = 0.16)$ and quasi-pinned connections $(\lambda_1 = \lambda_2 = 8.19)$. By inspection of Fig. 7, it is observed that the median (probability-based design value) and the average value (deterministic quantity) are largely different from each other. In particular, the average value of $\bar{s}_{11}$ is 0.49422 and represents the 89.51$^{\text{th}}$ percentile of the distribution (see the CDF depicted in Fig. 7(c)), whereas the median is 0.12772. This means that if one is dealing with the wide class of semi-rigid connections featured by $\lambda \in [0.16, 8.19]$, the element stiffness, on average, would be overestimated of around 125% by assuming the value calculated from the deterministic approach. Similar conclusions can be drawn for the $\bar{s}_{13}$ stiffness term, in which the median (0.071224) and the average value (0.40243) differ for up to 465%. In this case, the average value represents the 98.81$^{\text{th}}$ percentile of the distribution.

The peculiarity of a probability-based approach for semi-rigid connections is that a design value of the stiffness (and of any other quantity of interest for design purposes) that is related to a given non-exceeding probability (i.e., associated to a given limit state) can straightforwardly be identified. The probabilistic nature of the structural response can also be accounted for via the MCS. Nevertheless, only an approximation of the exact PDF may be obtained in this case: the number of samples needed to

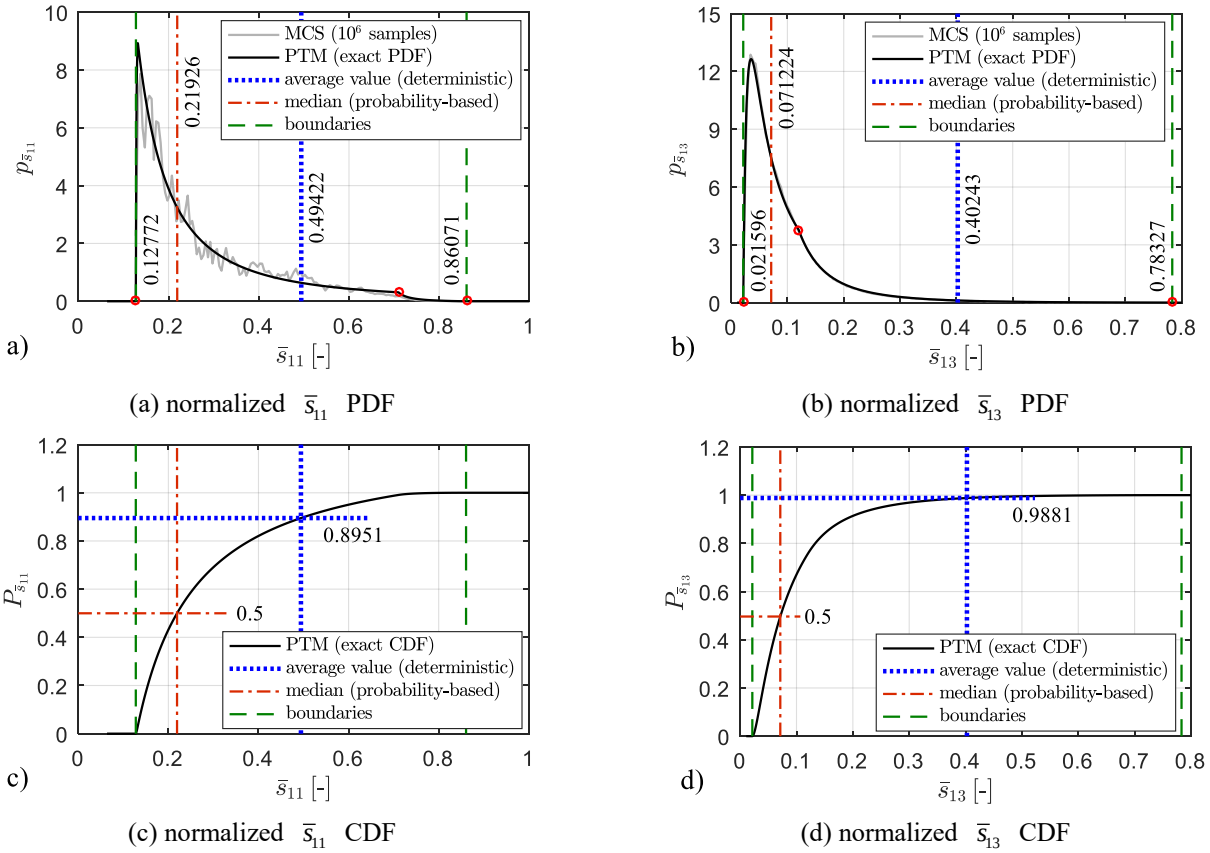

(a) normalized $\bar{s}_{11}$ PDF (b) normalized $\bar{s}_{13}$ PDF

(c) normalized $\bar{s}_{11}$ CDF (d) normalized $\bar{s}_{13}$ CDF

Fig. 7 Probabilistic response, in terms of rotational stiffness, of partially restrained beams: (a) normalized $\bar{s}_{11}$ PDF; (b) normalized $\bar{s}_{13}$ PDF; (c) normalized $\bar{s}_{11}$ CDF; (d) normalized $\bar{s}_{13}$ CDF

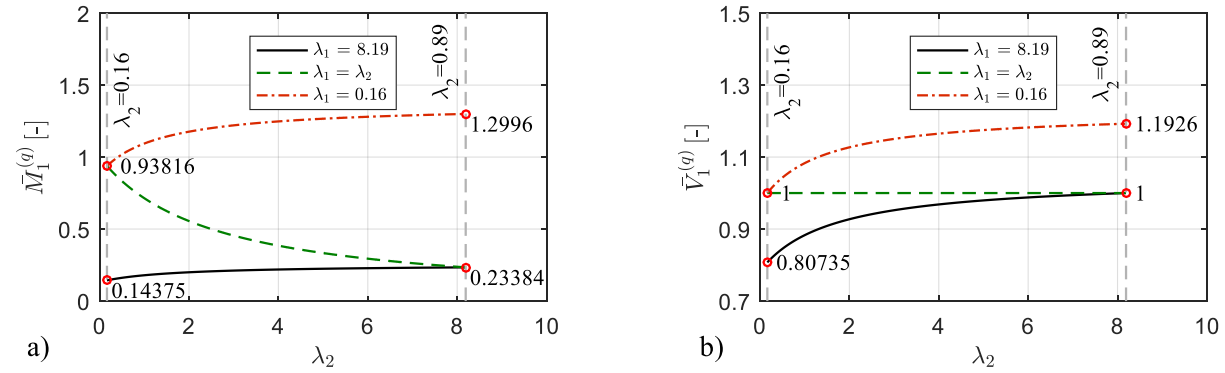

(a) $\bar{M}_1^{(q)}$ (b) $\bar{V}_1^{(q)}$

Fig. 8 Variability of the nodal reactions with the spring deformability terms: (a) $\bar{M}_1^{(q)}$; (b) $\bar{V}_1^{(q)}$

construct a reasonably accurate PDF exceeds millions, see again Fig. 7(a) and 7(b), which implies higher computational times. This concept is even more marked when the input-output relationship is nonlinear, as in the case of $\bar{s}_{11}$, cf. Eq. (32).

The PDF of the nodal reactions $\bar{M}_1^{(q)}$ and $\bar{V}_1^{(q)}$ of the partially restrained beam subject to a uniformly distributed load q is qualitatively different. Among the possible $\bar{M}_1^{(q)}$ values that may occur depending on the spring deformability λ_1 and λ_2, the minimum moment reaction (equal to 0.14375) occurs when λ_1=8.19 and λ_2=0.16, i.e., in the semi-rigid counterpart of a hinged-clamped beam idealization, whereas the maximum moment reaction (equal to 1.2996) takes place in the other way around for λ_1=0.16 and λ_2=8.19, i.e., in the semi-rigid approximation of a clamped-hinged beam, cf. Fig. 8. Other two characteristic points are detected in the $\bar{M}_1^{(q)}$ PDF, see Fig. 8(a): one is that for ($\bar{M}_1^{(q)} = 0.23384$, which corresponds to a cusp) and the other is for $\lambda_1 = \lambda_2 = 0.16$, $\bar{M}_1^{(q)} = 0.93816$.

In quite a similar way, the characteristic points of the

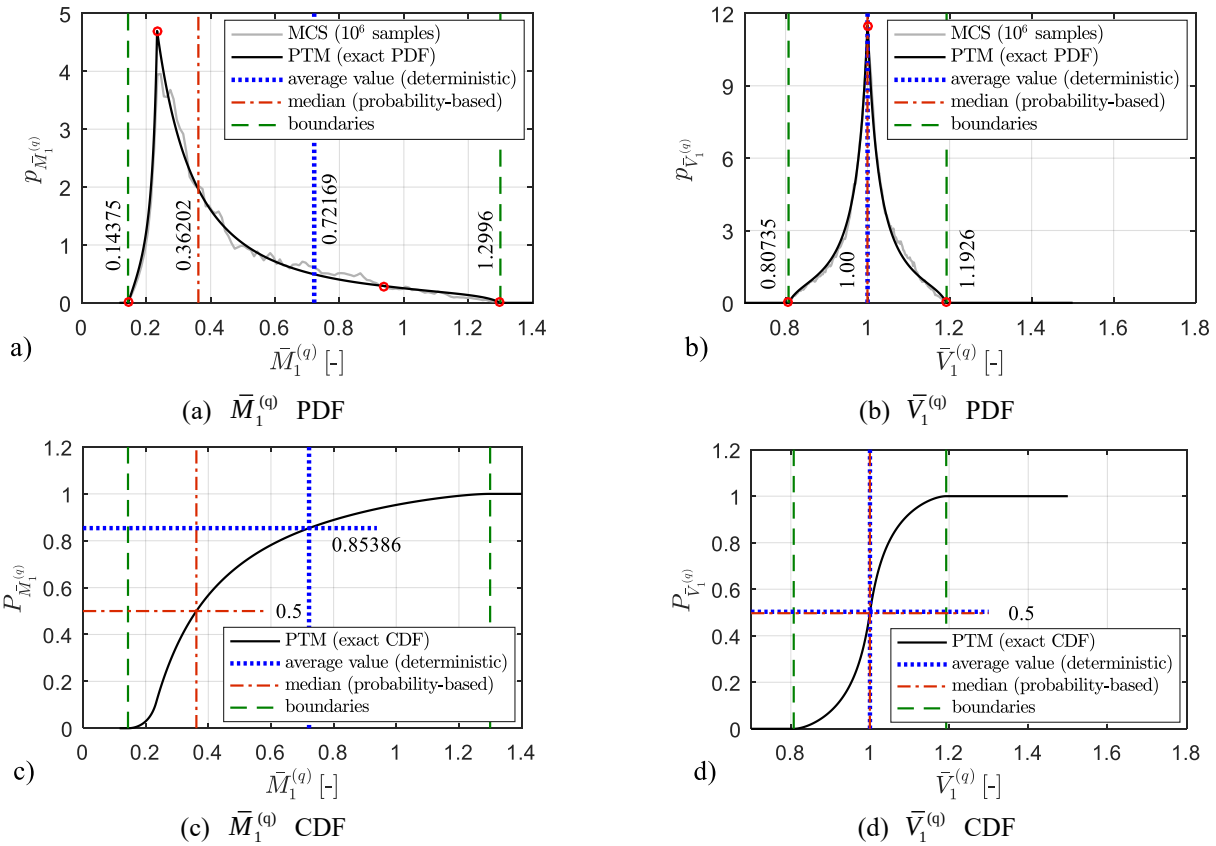

(a) $\bar{M}_1^{(q)}$ PDF (b) $\bar{V}_1^{(q)}$ PDF

(c) $\bar{M}_1^{(q)}$ CDF (d) $\bar{V}_1^{(q)}$ CDF

Fig. 9 Probabilistic response of partially restrained beams subject to a uniformly distributed load: (a) $\bar{M}_1^{(q)}$ PDF; (b) $\bar{V}_1^{(q)}$ PDF; (c) $\bar{M}_1^{(q)}$ CDF; (d) $\bar{V}_1^{(q)}$ CDF

transversal reaction $\bar{V}_1^{(q)}$ PDF are identified and associated to limit values of the λ_i values, cf. Fig. 8(b). As expected, deviations of $\bar{V}_1^{(q)}$ from the value $\bar{V}_1^{(q)}=1$ only occur when the two spring deformability terms are different from each other, i.e., for asymmetric beam restraints. Partially restrained beams with identical spring deformability at the two beam ends behave like clamped-clamped or hinged-hinged beams in terms of transversal nodal reactions. In the limit cases of quasi hinged-clamped (λ_1=8.19, λ_2=0.16) and quasi clamped-hinged beams (λ_1=0.16, λ_2=8.19) the extreme values of $\bar{V}_1^{(q)}$ are 0.80735 and 1.1926, respectively. The quantitative analysis of Fig. 9 reveals that the average value of the moment reaction (0.72169) represents the 85.39th of the distribution and deviates from the corresponding median value (0.36202) of 99.35%; on the contrary, due to the symmetric format of the $\bar{V}_1^{(q)}$ PDF, average and median values are coincident.

Finally, in Figs. 10 and 11, the mid-span bending moment $\bar{M}_0^{(q)}$ and the mid-span deflection $\bar{w}_0^{(q)}$ are characterized from a probabilistic point of view. These results are consistent with those of the stiffness terms, as the $\bar{M}_0^{(q)}$ and the $\bar{w}_0^{(q)}$ PDFs are both concentrated close to the quasi-pinned connection boundary (right side corresponding to λ_1=λ_2=8.19). The mid-span response is related to the overall deformability of the beam, therefore it is not affected by the specific values of λ_1 and λ_2 at the two end nodes individually considered, but rather it only depends on the sum λ_1+λ_2, which is physically reasonable. For instance, the same response in terms of bending moment and deflection would be obtained for λ_1=8.19, λ_2=0.16 and for λ_1=0.16, λ_2=8.19, cf. Fig. 10. Quantitative analysis of the $\bar{M}_0^{(q)}$ and the $\bar{w}_0^{(q)}$ PDFs, shown in Fig. 11, is of paramount importance from a design viewpoint: adopting the average (deterministic) value of mid-span moment and mid-span deflection means that the design is being carried out with the 19.42th and with the 19.41th percentile of the corresponding distribution, respectively. In other words, the deterministic approach would lead to assuming non-conservative (unsafe) estimates of mid-span moment and mid-span deflection that are lower than the median of the corresponding PDFs. In particular, the deterministic approach would underestimate the median of $\bar{M}_0^{(q)}$ by 15.26% and the median of $\bar{w}_0^{(q)}$ by 19.89%, respectively.

In Table 1, the main results of the present investigation are summarized. In particular, we report the two boundaries of the response indicators computed by assuming proper combinations of the two λ_1 and λ_2 deformability terms as discussed above.

The average value is the mean of these two bounds, which is compared to the median value. Considerable errors are found from this comparison, which alert the design

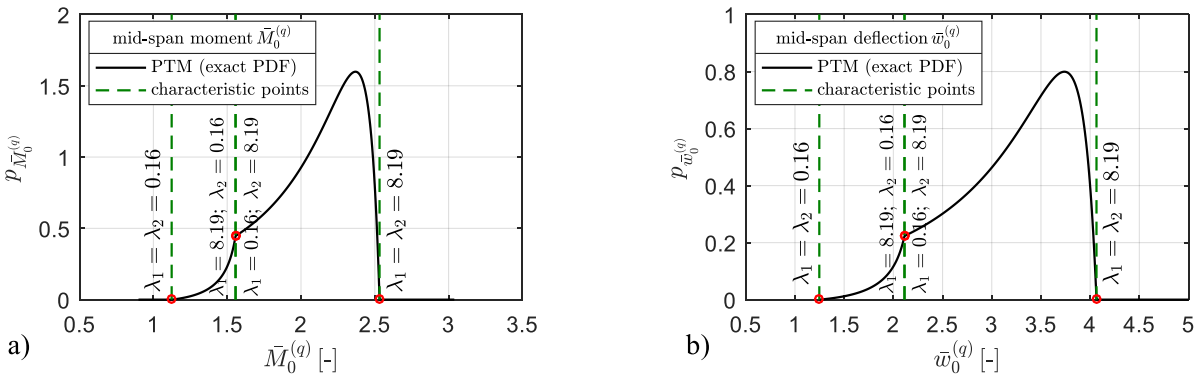

(a) $\bar{M}_0^{(q)}$ PDF (b) $\bar{w}_0^{(q)}$ PDF

Fig. 10 Qualitative examination of PDF of mid-span moment and mid-span deflection in partially restrained beams subject to a uniformly load q: (a) $\bar{M}_0^{(q)}$ PDF; (b) $\bar{w}_0^{(q)}$ PDF

Table 1 Probability-based approach versus deterministic approach for the design of beams with semi-rigid connections

response indicator	probability-based approach	deterministic approach				error (%)
	median (50th percentile)	lower bound	upper bound	average value	average percentile (%)	
$\bar{s}_{11}$	0.21926	2.62	2.53	3.34	2.67	2.46
$\bar{s}_{13}$	0.07122	0.021596	0.78327	0.40243	98.81	465.02
$\bar{M}_1^{(q)}$	0.36202	0.14375	1.2996	0.72169	85.39	99.35
$\bar{V}_1^{(q)}$	1.00	0.80735	1.1926	1.00	50.00	0.00
$\bar{M}_0^{(q)}$	2.1572	1.1237	2.5323	1.828	19.42	-15.26
$\bar{w}_0^{(q)}$	3.3152	1.2474	4.0646	2.656	19.41	-19.89

engineer that misleading outcomes may result from a deterministic approach applied to beams with partially restrained nodes if the fixity factors can be modelled as uniformly distributed random variables. These values, along with the PDFs illustrated above, could be employed to decide which value of rotational stiffness, mid-span deflection, bending moment (and so forth) to assume in a design process, and to assess which consequences such an assumption has from a probabilistic point of view.

It is worth noting that the above calculation considers a quite large spectrum of fixity factors, which encompasses the whole range of semi-rigid connections discussed in Section 2.3. However, as already noted in Section 2.3, when the type of connection is chosen for a steel framed structure, the range of variability of the fixity factor, and also of the spring deformability λ, is reduced as compared to the one assumed above, see e.g., (Abdalla and Chen 1995, Kim and Choi 2001). Which implications this restricted interval has in a design process is here briefly outlined.

To this aim, just as an example we suppose that a top-and-seat angle connection is adopted and a more realistic interval of λ is considered. Following the qualitative plot of Fig. 5(a), among the steel semi-rigid connections this quite flexible type of connection is close to the pinned EC3 connection boundary, therefore it has been characterized in terms of a λ_{ref}=7.0 value, assumed as a reference value in a design process. In line with the scope of the paper, in order to incorporate the largely scattered results that may arise from experiments, a ±50% deviation is assumed so that the λ variable is a uniformly distributed variable in the range $[0.5\lambda_{ref}, 1.5\lambda_{ref}]$. The probabilistic response of a beam complying with this more realistic assumption is illustrated in Fig. 12 in terms of mid-span bending moment $\bar{M}_0^{(q)}$ and deflection $\bar{w}_0^{(q)}$ PDF and CDF, respectively.

It is interesting to compare Fig. 11 with Fig. 12 that report the same results but arise from two different probabilistic characterizations of the beam-to-column connections. This comparison reveals that, as expected, the narrower interval of the λ values leads to a reduced variability of the response indicators. If the variation of λ were neglected and the calculation were performed assuming a deterministic λ_{ref}=7.0 value, a normalized moment and deflection equal to 2.391 and 3.7821 would be obtained (the average value in this case corresponds to the deterministic assumption $\lambda=\lambda_{ref}$). These values represent the 28.77th and 28.62th percentile of the corresponding distribution, respectively. Therefore, similar design implications to the above calculation are deduced, as the deterministic approach leads to non-conservative estimates of mid-span moment and mid-span deflection that are lower than the median of the corresponding PDFs. This result has been already obtained with the larger λ interval examined above. The underestimation is however less pronounced than the previous case with larger λ interval, and the associated relative error is reduced accordingly.

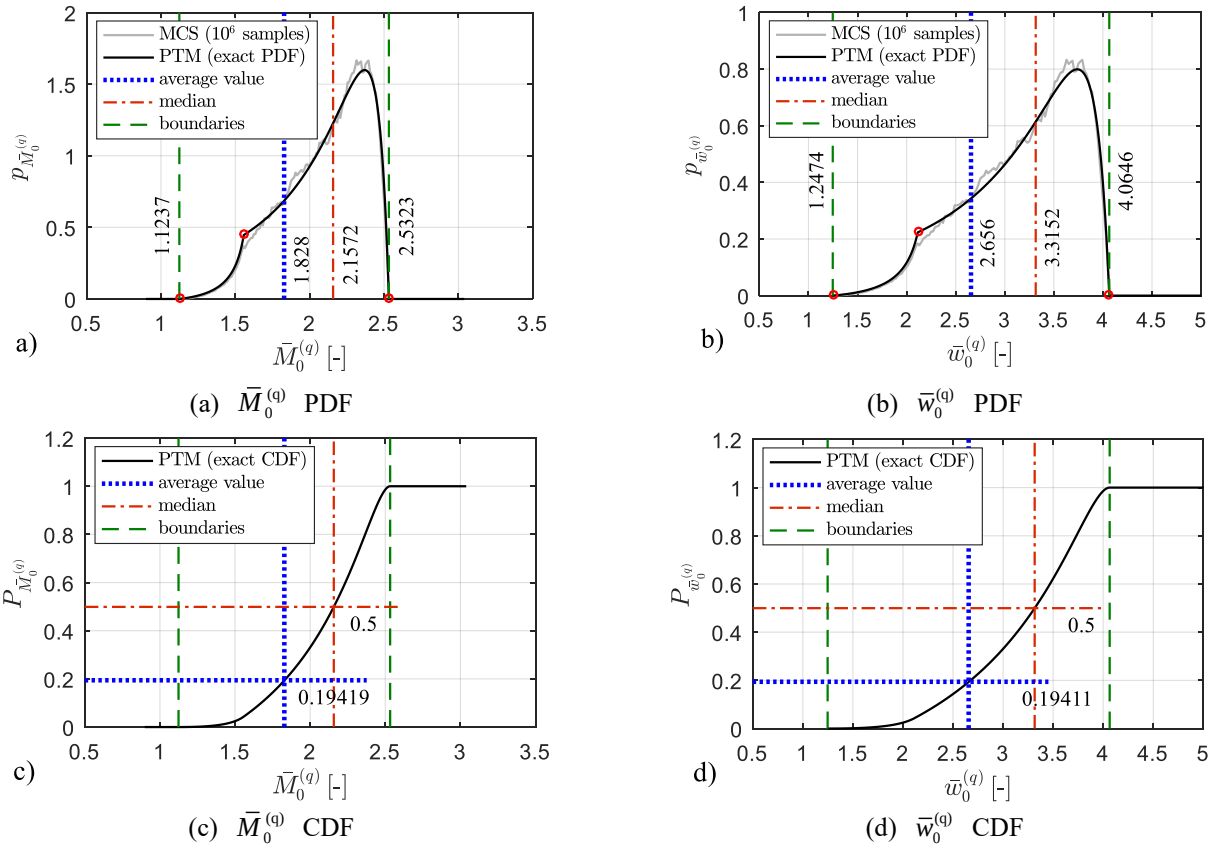

(a) $\bar{M}_0^{(q)}$ PDF (b) $\bar{w}_0^{(q)}$ PDF

(c) $\bar{M}_0^{(q)}$ CDF (d) $\bar{w}_0^{(q)}$ CDF

Fig. 11 Probabilistic response of partially restrained beams subject to a uniformly distributed load: (a) $\bar{M}_0^{(q)}$ PDF; (b) $\bar{w}_0^{(q)}$ PDF; (c) $\bar{M}_0^{(q)}$ CDF; (d) $\bar{w}_0^{(q)}$ CDF

Obviously, the higher is the dispersion, the more uncertain are the results. On the contrary, if λ were a deterministic variable, i.e., $\lambda=\lambda_{ref}$ without variation, all the response indicators would follow a Dirac Delta distribution centered at the average value and the probabilistic study here proposed would provide no added value as compared to a deterministic analysis. This underlines that the above conclusions are far from being of general validity, and the specific situation should be analyzed from case to case on the basis of available experimental data and input parameters (e.g., type of connections involved in a specific project).

5. Probabilistic response of frames with semi-rigid nodes

In this Section we present results concerning the probabilistic structural response of frames with semi-rigid connections. A single-bay frame with semi-rigid beam-to-column connections (frame I) and a single-bay frame with semi-rigid column-to-foundation connections (frame II) are investigated, as sketched in Fig. 4.

5.1 Single-bay frame with semi-rigid beam-to-column connections

The probabilistic response of the frame I subject to both a uniformly distributed load q applied on the BC partially restrained beam and a point load $P=qL$ applied to the node B is investigated. In Fig. 13, the PDF of node C rotation $\bar{\varphi}_C$ and lateral displacement $\bar{\delta}$ are illustrated. It is observed that when dealing with frames, due to the strongly nonlinear character of the relationships between the fixity factors and the response indicators (much higher than the individual beam, cf. Eqs. (17)), the number of samples needed to closely approximate the exact PDF by the MCS should be very high, largely exceeding one million. It is interesting to note that, due to the range of variability in the beam-to-column connection stiffness, a very large variability of the nodal rotations is expected, and the $\bar{\varphi}_C$ value may even change its sign as compared to the perfectly rigid case. However, this result is ascribed to the quite large assumed interval of fixity factors, as already noted above. Additionally, it is worth noting that in more realistic frames with a significant number of bays and floors, the influence of joint stiffness on the global response is certainly reduced as compared to this very simple frame structure with only one floor and one bay. In Fig. 14, the response in terms of moment reaction at the beam-to-column connection $\bar{M}_B$ and at the column base $\bar{M}_D$ is scrutinized from a probabilistic point of view. In line with the expectations, one million of samples in the MCS seems to be a satisfactory number for approximating the exact PDF of

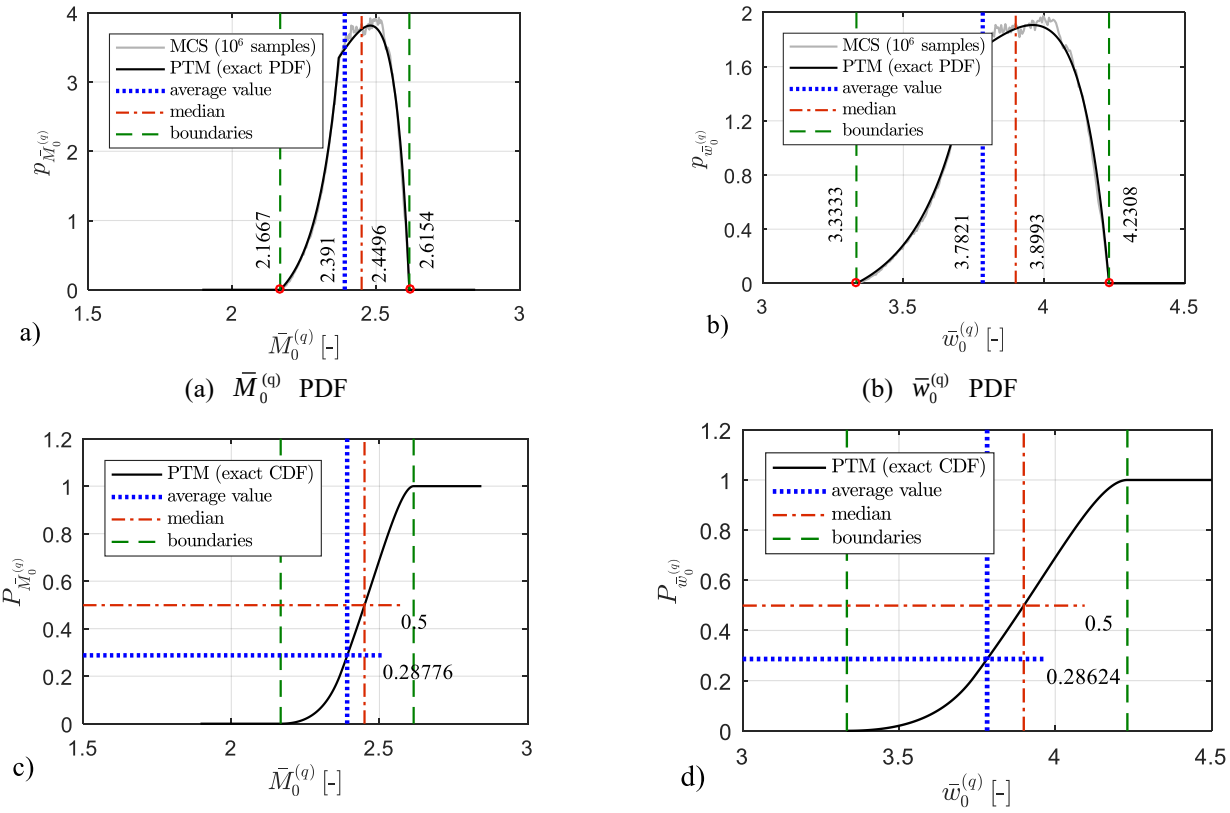

(a) $\bar{M}_0^{(q)}$ PDF (b) $\bar{w}_0^{(q)}$ PDF

(c) $\bar{M}_0^{(q)}$ CDF (d) $\bar{w}_0^{(q)}$ CDF

Fig. 12 Probabilistic response of beams with top-and-seat angle connections ($\lambda_{ref} = 7.0$, $\pm 50\%$ variation) subject to a uniform load: (a) $\bar{M}_0^{(q)}$ PDF; (b) $\bar{w}_0^{(q)}$ PDF; (c) $\bar{M}_0^{(q)}$ CDF; (d) $\bar{w}_0^{(q)}$ CDF

$\bar{M}_B$ but not that of $\bar{M}_D$ that involves a slightly more intricate relationship in terms of fixity factors, cf. Eqs. (19).

Average and median $\bar{M}_B$ values differ for almost 300%, which means that a design based on the average value would disproportionally overestimate the design moment at the node *B*. Indeed, the average value (0.41476) represents the 91.68th percentile of the $\bar{M}_B$ distribution. Moreover, a small influence of the semi-rigid connections on the moment at the column base $\bar{M}_D$ is detected, which is physically consistent as the randomness is concentrated on the beam and not on the column. Indeed, the variability of $\bar{M}_D$ is comprised to within nearly a $\pm 7\%$ of the perfectly-rigid case, with extreme values equal to 0.94051 and 1.0704 corresponding to the couples $(\lambda_1 = 8.19, \lambda_2 = 0.16)$ and $(\lambda_1 = \lambda_2 = 8.19)$, respectively. Owing to the narrow interval in which the $\bar{M}_D$ PDF is concentrated and considering the $\bar{M}_B$ PDF, it can be concluded that deterministic approaches would lead to reasonable approximations of the moment reaction at the column base but not of the moment reaction at the beam-to-column connection.

5.2 Single-bay frame with semi-rigid column-to-foundation connections

The probabilistic response of the single-bay frame with semi-rigid column-to-foundation connections is finally sought. By inspection of Fig. 15, it emerges that in this case the moment reaction $\bar{M}_D$ PDF at the column base is not confined to within a rather narrow interval, as in the previous frame, but is widely distributed and extends from 0.33053 to 0.94913. This is physically consistent, because in this case the randomness of the connection concerns just the base of the columns, therefore in contrast to the previous case the fixity factors lead to a significant variability of the $\bar{M}_D$ value. The deterministic average values of $\bar{M}_B$ and $\bar{M}_D$ represent the 72.05th and the 77.18th percentile of the distribution, respectively. Therefore, in this case resorting to a probabilistic design approach would lead to more economical solutions, based on lower moments at both the beam-to-column connection and at the column base. The peculiar interval-like trend of the $\bar{M}_B$ and $\bar{M}_D$ PDFs shown in Fig. 15(a) and 15(b) is just a consequence of the uniform distribution assumption of the fixity factors. It seems interesting to scrutinize to what extent the probability-based structural response varies if a different assumption were made on the probabilistic distribution of the fixity factors.

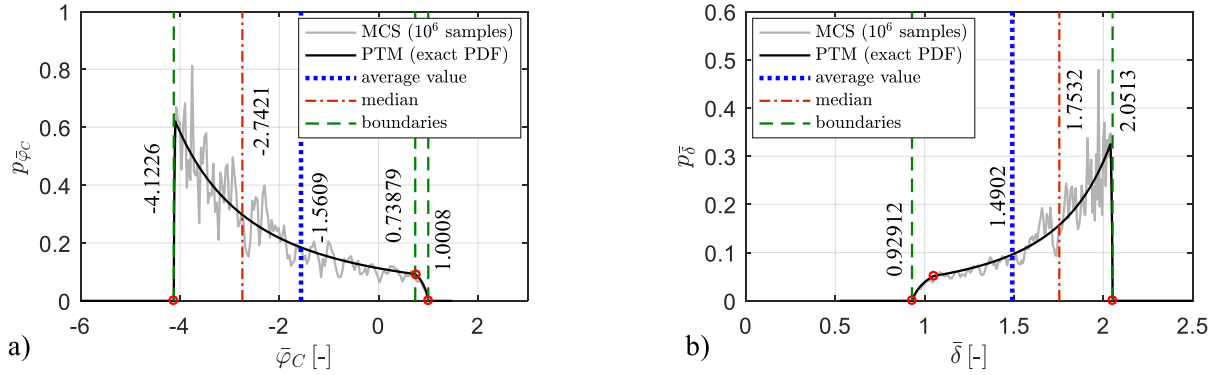

(a) $\bar{\varphi}_C$ PDF (b) $\bar{\delta}$ PDF

Fig. 13 Probabilistic response of frame I with semi-rigid beam-to-column connections: (a) normalized $\bar{\varphi}_C$ PDF; (b) normalized $\bar{\delta}$ PDF

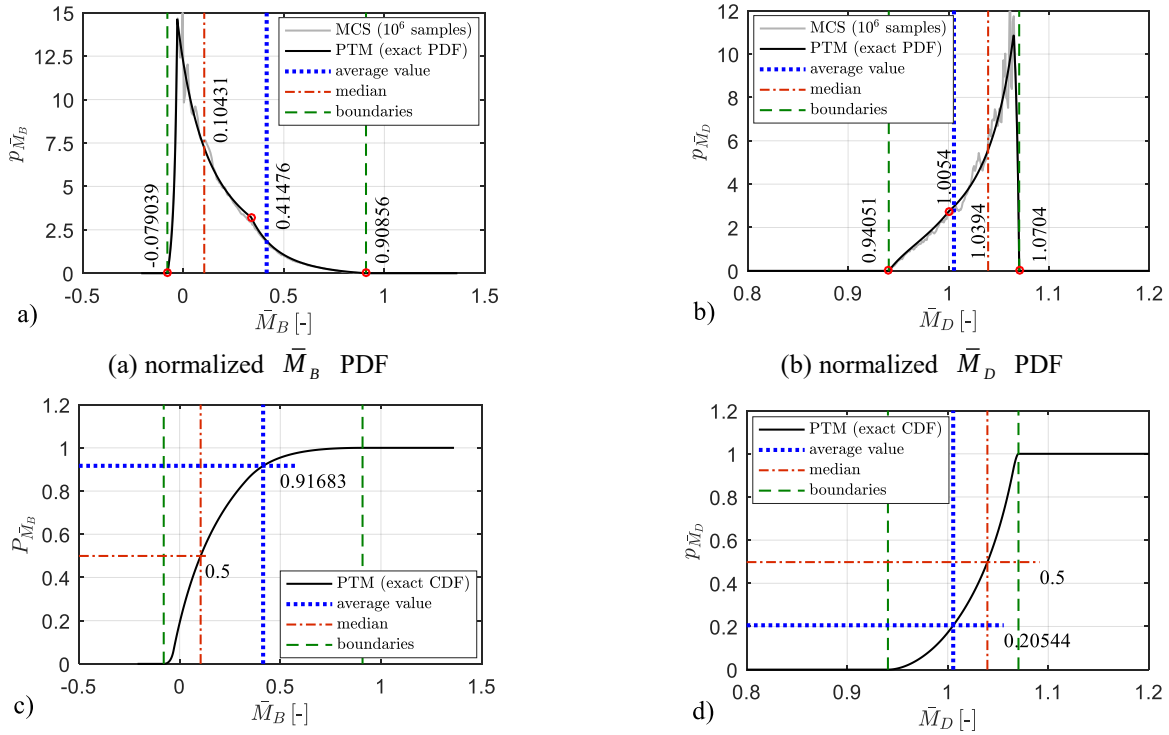

(a) normalized $\bar{M}_B$ PDF (b) normalized $\bar{M}_D$ PDF

(c) normalized $\bar{M}_B$ CDF (d) normalized $\bar{M}_D$ CDF

Fig. 14 Probabilistic response of frame I with semi-rigid beam-to-column connections: (a) normalized $\bar{M}_B$ PDF; (b) normalized $\bar{M}_D$ PDF; (c) normalized $\bar{M}_B$ CDF; (d) normalized $\bar{M}_D$ CDF

To this aim, in Fig. 16, we report the $\bar{M}_B$ and $\bar{M}_D$ PDFs by assuming that the fixity factors follow a lognormal distribution in place of a uniform distribution. The parameters of the lognormal distribution have been selected according to the following criterion

$$\mu = \frac{0.16+8.19}{2} = 0.525; \qquad \mu_{\log} = 1.4297; \quad \sigma = \frac{0.16+8.19}{10} = 0.835527 \tag{33}$$

Although the PDFs of $\bar{M}_B$ and $\bar{M}_D$ resulting from the lognormal distribution are qualitatively different from those of Fig. 15, these distributions leads to really similar considerations from a design viewpoint: for instance, the median of $\bar{M}_B$ is -1.2031 against the value -1.1978 found for a uniform distribution. Other relevant comparisons are listed in Table 2. This comparison highlights that the results discussed in this paper can be considered of quite general validity, since they are little affected by the choice of the fixity factors distribution. Obviously, the design engineer should carefully reflect upon this assumption and should

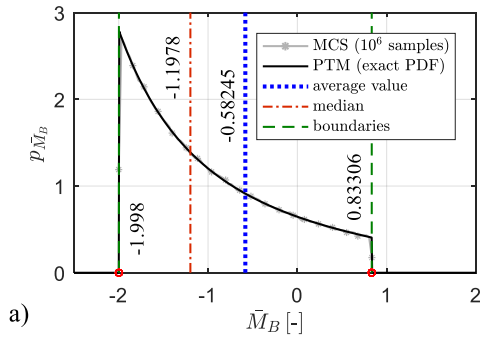

(a) normalized $\bar{M}_B$ PDF

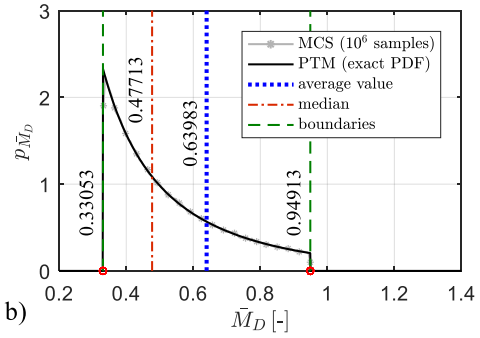

(b) normalized $\bar{M}_D$ PDF

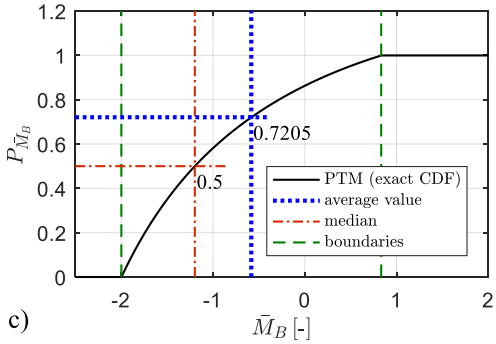

(c) normalized $\bar{M}_B$ CDF

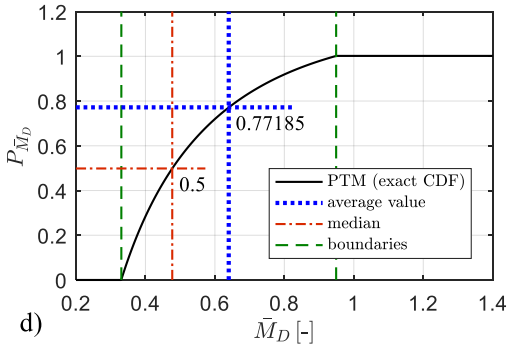

(d) normalized $\bar{M}_D$ CDF

Fig. 15 Probabilistic response of frame II with semi-rigid column-to-foundation connections: (a) normalized $\bar{M}_B$ PDF; (b) normalized $\bar{M}_D$ PDF; (c) normalized $\bar{M}_B$ CDF; (d) normalized $\bar{M}_D$ CDF

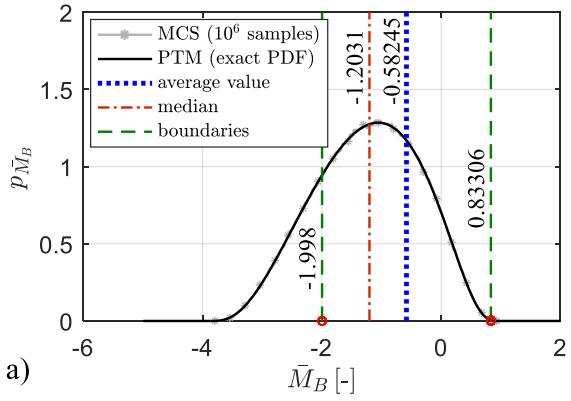

(a) $\bar{M}_0^{(q)}$ PDF

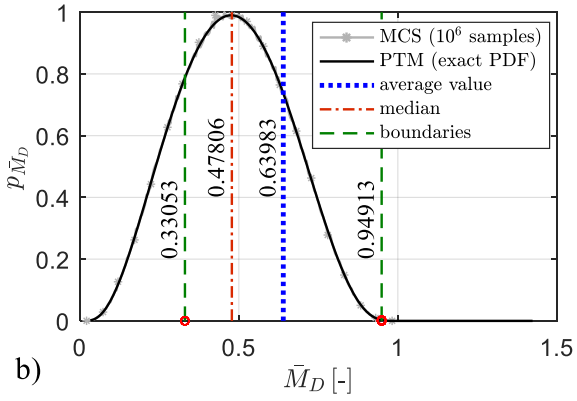

(b) $\bar{w}_0^{(q)}$ PDF

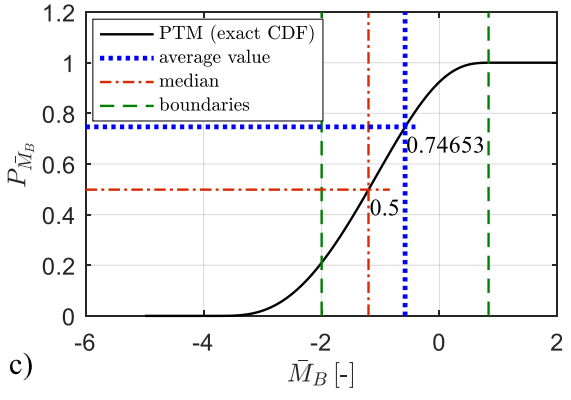

(c) $\bar{M}_0^{(q)}$ CDF

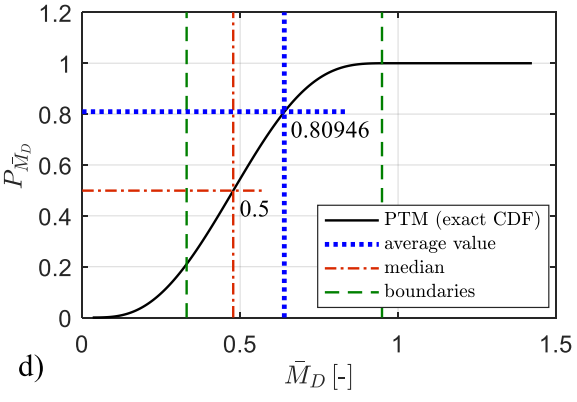

(d) $\bar{w}_0^{(q)}$ CDF

Fig. 16 Same as Fig. 15 but with a lognormal distribution assumption for the fixity factors

Table 2 Probability-based approach versus deterministic approach for the design of beams with semi-rigid connections

response indicator	uniform distribution for fixity factors		lognormal distribution for fixity factors	
	median (50^{th} percentile)	average value percentile (%)	median (50^{th} percentile)	average value percentile (%)
$\bar{M}_B$	-1.1978	72.05	-1.2031	74.65
$\bar{M}_D$	0.47713	77.18	0.47806	80.94

adopt the most appropriate fixity factors distribution on the basis of available experimental data regarding the specific semi-rigid connections involved in the project.

6. Conclusions

A fully probabilistic approach has been presented to describe the structural response of steel beams and frames with uncertain semi-rigid connections. The non-perfect constraints and joints are endowed of an uncertain degree of rotational stiffness, through the definition of the deformability of the springs via random variables. Incidentally, closed-form expressions of a few structural response indicators of beams and simple frames with partially restrained nodes have been presented. The randomness of the structural response has been entirely ascribed to the uncertainty in the fixity factors at the beam end nodes, thus related to the rotational deformability of the springs. The adopted probabilistic approach, based on the application of the PTM to vector-valued random variables related by means of the nonlinear laws above cited, permits one to compute the exact PDF of the structural response based on the distribution of the fixity factors. Therefore, the design engineer can straightforwardly identify the value of certain indicators of the structural response associated to a given non-exceeding probability, which is very important in the framework of limit state design. The characterization of the rotational spring stiffness terms should be based upon experimental findings and laboratory calibration, which is beyond the scope of the proposed analytical study. In this paper, reference has been made to the EC3 provisions, wherein limit values of the fixity factors for steel semi-rigid connections are indicated. We have reasonably assumed that the fixity factors are uniformly distributed within such EC3 interval, although the proposed analysis method is applicable to a more general class of elements and materials, not confined to steel framed structures. The PDFs of a few indicators of the structural response have been derived for both beams and simple frames.

Design considerations have emerged when comparing the probability-based approach with a deterministic approach based on the average values, the latter referring to the intermediate values of the fixity factors between the two extreme cases. Misleading (and in some cases non-conservative) conclusions from a design viewpoint might be drawn unless the probabilistic nature of the structural response is properly accounted for, i.e., when resorting to a deterministic approach. As an example, if the deterministic average values were assumed in the design process, one would underestimate the mid-span deflection of around 20% and, similarly, the mid-span bending moment of nearly 15% as compared to the median (probability-based) value.

However, there is not a unified and common trend for all the response indicators, for instance some response quantities such as the moment reaction at the joint, are overestimated and not underestimated. In the authors' opinion, more reliable reactions and deflections than those derived from a deterministic approach are however obtained, which leads to more realistic and economical design decisions especially when experimental data on the connection stiffness are quite scattered.

Although the design engineer could decide to select more appropriate distributions than the uniform on the basis of available experimental data, it has been observed that the obtained results are little affected by the distribution itself. On the contrary, it is of relevant importance to identify appropriate upper bounds and lower bounds of the fixity factors for the given connections (that are element-specific and material-specific data) involved in a given structure, which falls beyond the scope of the present paper. In this regard, literature review papers as well as experimental testing should assist the designer in such choice. With no doubt, the range of variability of the fixity factors alters the outcomes of the probability-based investigation. In many practical cases, this range is narrower than the interval adopted in this paper, especially because the type of connection is known in a framed structure. However, the general qualitative conclusions drawn for the quite large interval adopted in this paper remain, as demonstrated by the analysis of a more reasonable case in which a specific connection type has been selected and a more realistic interval has been considered. Rather than providing precise probabilistic results for each specific connection type, the aim of this paper is just limited to present a more accurate method of analysis and to alert the engineer that certain design implications arise when resorting to a non-probabilistic (deterministic) design approach. Semi-rigid connections, by nature characterized by largely scattered results, should be more appropriately dealt with via a fully probabilistic approach.

Acknowledgments

The financial support from the Italian Ministry of Education, University and Research (PRIN Grant 015TTJN95 and PRIN Grant 2015JW9NJT) is gratefully acknowledged.

References

Abdalla, K.M. and Chen, W.F. (1995), "Expanded database of semirigid steel connections", *Comput. Struct.*, **56**(4), 553-564.

Adhikari, S. and Manohar, C.S. (1999), "Dynamic analysis of framed structures with statistical uncertainties", *Int. J. Numer. Meth. Eng.*, **44**(8), 1157-1178.

Agel, P. and Lokaj, A. (2014), "Semi-rigid joint of timber-concrete composite beams with steel plates and convex nails", *Wood Res.*, **59**(3), 491-498.

AISC (American Institute of Steel Construction) (1994), *LRFD, Manual of Steel Construction, Load and Resistance Factor Design*, 2nd Edition, Chicago, U.S.A.

Amadio, C., Moschino, D. and Fragiacomo, M. (2006), *Probabilistic Analysis of a PR Steel-Concrete Composite Frame*, In *STESSA 2006*-Mazzolani & Wada (eds.), Taylor & Francis Group, London, U.K.

Artar, M. and Daloglu, A.T. (2015), "Optimum design of steel frames with semi-rigid connections and composite beams", *Struct. Eng. Mech.*, **55**(2), 299-313.

Basaga, H.B., Kartal, M.E. and Bayraktar, A. (2012), "Reliability analysis of steel braced reinforced concrete frames with semi-rigid connections", *Int. J. Struct. Stab. Dyn.*, **12**(5), 1250037 1-20.

Bathe, K.J. (1996), *Finite Element Procedures*, Prentice-Hall, New Jersey, U.S.A.

Bjorhovde, R., Colson, A. and Brozzetti, J. (1990), "Classification system for beam-to-column connections", *J. Struct. Eng.*, **116**(11), 3059-3076.

Çavdar, Ö., Bayraktar, A., Çavdar, A. and Kartal, M.E. (2009), "Stochastic finite element analysis of structural systems with partially restrained connections subjected to seismic loads", *Steel Compos. Struct.*, **9**(6), 499-518.

CEN (European Committee for Standardization) (2005), *EN 1993-1-1, Eurocode 3: Design of Steel Structures-Part 1-1: General Rules and Rules for Buildings*, Brussels, Belgium.

Chen, W.F. and Lui, E.M. (1987), "Effects of joint flexibility on the behavior of steel frames", *Comput. Struct.*, **26**(5), 719-732.

Chen, W.F., Kishi, N. and Komuro, M. (2011), *Semi-Rigid Connections Handbook*, J. Ross Publishing.

Chiorean, C.G. (2009), "A computer method for nonlinear inelastic analysis of 3D semi-rigid steel frameworks", *Eng. Struct.*, **31**, 3016-3033.

Csébfalvi, A. (2007), "Optimal design of frame structures with semi-rigid joints", *Per. Polytech.*, **51**(1), 9-15.

De Domenico, D., Falsone, G. and Settineri, D. (2018), "Probabilistic buckling analysis of beam-column elements with geometric imperfections and various boundary conditions", *Meccan.*, **53**(4-5), 1001-1013.

De Domenico, D., Fuschi, P., Pardo, S. and Pisano, A.A. (2014), "Strengthening of steel-reinforced concrete structural elements by externally bonded FRP sheets and evaluation of their load carrying capacity", *Compos. Struct.*, **118**, 377-384.

Esfandyary, R., Razzaghi, M.S., Eslami, A. and Branch, T. (2015), "A parametric investigation on the hysteretic behaviour of CFT column to steel beam connections", *Struct. Eng. Mech.*, **55**(1), 205-228.

Faella, C., Martinelli, E. and Nigro, E. (2008), "Analysis of steel-concrete composite PR-frames in partial shear interaction: A numerical model and some applications", *Eng. Struct.*, **30**, 1178-1186.

Falsone, G. and Settineri, D. (2013a), "Explicit solutions for the response probability density function of linear systems subjected to random static loads", *Prob. Eng. Mech.*, **33**, 86-94.

Falsone, G. and Settineri, D. (2013b), "Explicit solutions for the response probability density function of nonlinear transformations of static random inputs", *Prob. Eng. Mech.*, **33**, 79-85.

Görgün, H. (1997), "Semi-rigid behaviour of connections in precast concrete structures", Ph.D. Dissertation, University of Nottingham, U.K.

Gorgun, H. and Yilmaz, S. (2012), "Geometrically nonlinear analysis of plane frames with semi-rigid connections accounting for shear deformations", *Struct. Eng. Mech.*, **44**(4), 539-569.

Graham, A. (1981), *Kronecker Products and Matrix Calculus with Applications*, Ellis Horwood Limited, Chichester, U.K.

Hadianfard, M.A. and Razani, R. (2003), "Effects of semi-rigid behavior of connections in the reliability of steel frames", *Struct. Safety*, **25**, 123-138.

Hadidi, A. and Rafiee, A. (2014), "Harmony search based, improved particle swarm optimizer for minimum cost design of semi-rigid steel frames", *Struct. Eng. Mech.*, **50**(3), 323-347.

Jones, S.W., Kirby, P.A. and Nethercot, D.A. (1983), "The analysis of frames with semi-rigid connections-a state-of-the-art report", *J. Constr. Steel Res.*, **3**(2), 2-13.

Kartal, M.E., Başağa, H.B., Bayraktar, A. and Muvafik, M. (2010), "Effects of semi-rigid connection on structural responses", *Electr. J. Struct. Eng.*, **10**, 22-35.

Katkhuda, H.N., Dwairi, H.M. and Shatarat, N. (2010), "System identification of steel framed structures with semi-rigid connections", *Struct. Eng. Mech.*, **34**(3), 351.

Kim, S.E. and Choi, S.H. (2001), "Practical advanced analysis for semi-rigid space frames", *Int. J. Sol. Struct.*, **38**(50), 9111-9131.

Kishi, N. and Chen, W.F. (1990), "Moment-rotation relations of semirigid connections with angles", *J. Struct. Eng.*, **116**(7), 1813-1834.

Larsen, H.J. and Jensen, J.L. (2000), "Influence of semi-rigidity of joints on the behaviour of timber structures", *Progr. Struct. Eng. Mater.*, **2**(3), 267-277.

Lutes, L.D. and Sarkani, S. (2004), *Random Vibration Analysis of Structural and Mechanical System*, Burlington, U.S.A.

Nie, J., Tao, M., Cai, C.S. and Chen, G. (2011), "Modeling and investigation of elasto-plastic behavior of steel-concrete composite frame systems", *J. Constr. Steel Res.*, **67**, 1973-1984.

Papoulis, A. and Pillai, S.U. (2002), *Probability, Random Variables, and Stochastic Processes*, 4th Edition, McGraw-Hill.

Pisano, A.A., Fuschi, P. and De Domenico, D. (2014), "Limit state evaluation of steel-reinforced concrete elements by von Mises and Menétrey-Willam-type yield criteria", *Int. J. Appl. Mech.*, **6**(05), 1450058.

Pisano, A.A., Fuschi, P. and De Domenico, D. (2015), "Numerical limit analysis of steel-reinforced concrete walls and slabs", *Comput. Struct.*, **160**, 42-55.

Rauscher, T.R. and Gerstle, K.H. (1992), "Reliability of rotational behavior of framing connections", *Eng. J. AISC*, **29**(1), 12-19.

Sakurai, S., Ellingwood, B.R. and Kushiyama, S. (2001), "Probabilistic study of the behavior of steel frames with partially restrained connections", *Eng. Struct.*, **23**, 1410-1417.

Sekulovic, M. and Salatic, R. (2001), "Nonlinear analyses of frames with flexible connections", *Comput. Struct.*, **79**, 1097-1107.

Simões, L.M.C. (1996), "Optimization of frames with semi-rigid connections", *Comput. Struct.*, **60**(4), 531-539.

Tangaramvong, S., Tin-Loi, S., Yang, C. and Gao, W. (2016), "Interval analysis of nonlinear frames with uncertain connection properties", *Int. J. Non-Lin. Mech.*, **86**, 83-95.

Thai, H.T., Uy, B., Kang, W.H. and Hicks, S. (2016), "System reliability evaluation of steel frames with semi-rigid connections", *J. Constr. Steel Res.*, **121**, 29-39.

Zohra, D.F. and Nacer, T.A. (2018), "Dynamic analysis of steel frames with semi-rigid connections", *Struct. Eng. Mech.*, **165**(3), 327-334.

CC